Journal of African Earth Sciences 70 (2012) 36–57

Contents lists available at SciVerse ScienceDirect

Journal of African Earth Sciences

journal homepage: www.elsevier.com/locate/jafrearsci

Lithostratigraphy, biostratigraphy and chemostratigraphy of Upper Cretaceous and Paleogene sediments from southern Tanzania: Tanzania Drilling Project Sites 27–35

Àlvaro Jimènez Berrocoso [a,*], Brian T. Huber [b], Kenneth G. MacLeod [c], Maria Rose Petrizzo [d], Jacqueline A. Lees [e], Ines Wendler [b], Helen Coxall [f], Amina K. Mweneinda [f], Francesca Falzoni [d], Heather Birch [f], Joyce M. Singano [g], Shannon Haynes [c], Laura Cotton [f], Jens Wendler [b], Paul R. Bown [e], Stuart A. Robinson [e], Jeremy Gould [e]

[a] School of Earth, Atmospheric and Environmental Sciences, University of Manchester, Oxford Road, Manchester M13 9PL, UK
[b] Department of Paleobiology, MRC 121, Smithsonian Museum of Natural History, Washington, DC 20013-7012, USA
[c] Department of Geological Sciences, University of Missouri, Columbia, MO 65211, USA
[d] Dipartimento di Scienze della Terra "Ardito Desio", Università degli Studi Milano, via Mangiagalli, Milan, Italy
[e] Department of Earth Sciences, University College London, Gower Street, London WC1E 6BT, UK
[f] School of Earth, Ocean and Planetary Sciences, Cardiff University, Park Place, Cardiff CF10 3YE, UK
[g] Tanzania Petroleum Development Corporation, PO Box 2774, Dar es Salaam, Tanzania

ARTICLE INFO

Article history:
Received 23 November 2011
Received in revised form 18 May 2012
Accepted 30 May 2012
Available online 9 June 2012

Keywords:
Tanzania Drilling Project
Kilwa Group
Upper Cretaceous biostratigraphy
Turonian glassy foraminifera
Holococcoliths
Cretaceous–Paleogene boundary

ABSTRACT

The 2008 Tanzania Drilling Project (TDP) expedition recovered common planktonic foraminifera (PF), calcareous nannofossils (CN) and calcareous dinoflagellates with extraordinary shell preservation at multiple Cenomanian–Campanian sites that will be used for paleoclimatic, paleoceanographic, and biostratigraphic studies. New cores confirm the existence of a more expanded and continuous Upper Cretaceous sequence than had previously been documented in the Lindi and Kilwa regions of southeastern coastal Tanzania. This TDP expedition cored 684.02 m at eight Upper Cretaceous sites (TDP Sites 28–35) and a thin Paleocene section (TDP Site 27).

TDP Sites 29, 30, 31 and 34 together span the lowermost Turonian to Coniacian (PF *Whiteinella archaeocretacea* to *Dicarinella concavata* Zones and CN Zones UC6a–9b), with TDP Site 31 being the most biostratigraphically complete Turonian section found during TDP drilling. A discontinuous section from the Santonian–upper Campanian (PF *D. asymetrica* to *Radotruncana calcarata* Zones and CN Zones UC12–16) was collectively recovered at TDP Sites 28, 32 and 35, while thin sequences of the lower Cenomanian (PF *Thalmanninella globotruncanoides* Zone and CN subzones UC3a–b) and middle Paleocene (Selandian; PF Zone P3a and CN Zone NP5) were cored in TDP Sites 33 and 27, respectively. Records of $\delta^{13}C_{org}$ and $\delta^{13}C_{carb}$ from bulk sediments generated for all the Cretaceous sites show largely stable values through the sections. Only a few parallel $\delta^{13}C_{org}$ and $\delta^{13}C_{carb}$ shifts have been found and they are interpreted to reflect local processes. The $\delta^{18}O_{carb}$ record, however, is consistent with Late Cretaceous cooling trends from the Turonian into the Campanian. Lithologies of these sites include thick intervals of claystones and siltstones with locally abundant, finely-laminated fabrics, irregular occurrences of thin sandstone layers, and sporadic bioclastic debris (e.g., inoceramids, ammonites). Minor lithologies represent much thinner units of up to medium-grained, massive sandstones. The $\%CaCO_3$ (~5–40%) and $\%C_{org}$ (~0.1–2%) are variable, with the highest $\%CaCO_3$ in the lower Campanian and the highest $\%C_{org}$ in the Turonian. Lithofacies analysis suggests that deposition of these sediments occurred in outer shelf-upper slope, a setting that agrees well with inferences from benthic foraminifera and calcareous dinoflagellates.

1. Introduction

The southeastern coast of Tanzania is well known for the occurrence of exceptionally well-preserved calcareous microfossils in Upper Cretaceous–Neogene shelfal facies (Pearson et al., 2004, 2006; Bown, 2005; Lees, 2007; Bown et al., 2008; Jiménez Berrocoso et al., 2010). Relatively impermeable, clay-rich sediments and shallow burial depths have been proposed to explain this excellent preservation (e.g., Pearson et al., 2004, 2006; Nicholas et al., 2006, 2007). In addition, remarkably diverse microfossil assemblages have been found in these sediments (Pearson et al., 2001; Bown,

* Corresponding author.
E-mail address: alvaro.jimenezberrocoso@manchester.ac.uk (À. Jimènez Berrocoso).

1464-343X/$ - see front matter © 2012 Elsevier Ltd. All rights reserved.
http://dx.doi.org/10.1016/j.jafrearsci.2012.05.006

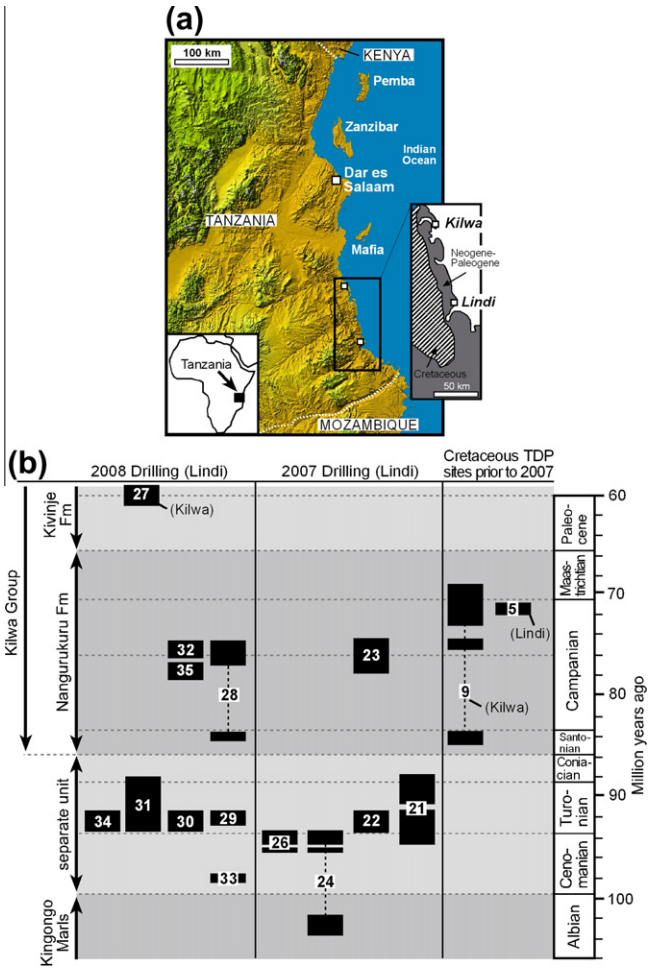

Fig. 1. (a) Location of Cretaceous and Paleogene–Neogene sediments between Kilwa and Lindi in southeastern coastal Tanzania. (b) Stratigraphic extent of the TDP sites drilled prior to 2007 and in 2007–2008, together with main stratigraphic units.

2005; Bown and Dunkley Jones, 2006; Lees, 2007; Bown et al., 2008; Petrizzo et al., 2011; Falzoni and Petrizzo, 2011; Wendler et al., 2011), which together makes this region crucial to advancing our understanding of the low-latitude biostratigraphy and biodiversity of the Late Cretaceous–Neogene, as well as to the study of subtropical–tropical temperature records.

Since 2002, the Tanzania Drilling Project (TDP) has targeted outcrop and core sediment samples from southeastern coastal Tanzania and examined exceptionally well-preserved foraminifera and calcareous nannofossils for Upper Cretaceous to Neogene biostratigraphic and paleoclimatic studies (Pearson et al., 2001, 2007, 2008; Stewart et al., 2004; Handley et al., 2008; Petrizzo et al., 2011; Wendler et al., 2011). The first phase of TDP field mapping and subsurface studies redefined the lithostratigraphy (Nicholas et al., 2006), structural geology (Nicholas et al., 2007) and biostratigraphic ages (Pearson et al., 2004, 2006) for the Campanian–Oligocene succession between Kilwa and Lindi (Fig. 1a), as well as provided new organic geochemical data (van Dongen et al., 2006). The second phase of drilling, beginning in 2007 near Lindi, however, showed the existence of a more stratigraphically expanded Upper Cretaceous section than had been appreciated in previous studies (Jiménez Berrocoso et al., 2010). In addition, stable isotopic evidence for partial recovery of Ocean Anoxic Event 2, close to the Cenomanian–Turonian boundary, was found in several drilled sites (Jiménez Berrocoso et al., 2010).

In this paper, we provide a litho-, bio- and chemostratigraphic synthesis of the 2008 drilling season near Lindi and Kilwa, which yielded a total of 684.02 m of core from the lower Cenomanian to the upper Campanian (TDP Sites 28–35), along with a thin middle Paleocene section (TDP Site 27). Our results confirm that this area exhibits an expanded and nearly complete Upper Cretaceous succession yielding exquisitely preserved microfossils in most intervals. Detailed study of the microfossil assemblages will significantly advance our understanding of the biostratigraphy, biodiversity, paleoclimate and paleoceanography of the subtropical Indian Ocean during the Late Cretaceous.

2. Geological setting

A thick sequence of marine claystones and siltstones, spanning the middle Cretaceous–Neogene, occur to the south of Dar es Salaam, with a strike that is mostly parallel to the coastline and a shallow oceanward dip (Nicholas et al., 2007). The most extensive and accessible exposures are located in a continuous band between Kilwa and Lindi (Moore et al., 1963; Kent et al., 1971; Gierlowski-Kordesch and Ernst, 1987; Ernst and Schlüter, 1989; Ernst and Zander, 1993) (Fig. 1a). For further descriptions of the regional geology and tectonic setting see Salman and Abdula (1995), Pearson et al. (2004), Nicholas et al. (2006, 2007) and Key et al. (2008).

2.1. Upper Cretaceous sediments

Schlüter (1997) named the Kilwa Group for the Upper Cretaceous sediments exposed around Kilwa, but no specific formations or stratigraphic boundaries were defined. Nicholas et al. (2006) proposed that between Kilwa and Lindi the Santonian–Maastrichtian sediments of the Nangurukuru Formation (Fm.) belong to the base of the Kilwa Group (Fig. 1b). Sediments from this interval consist of silty claystones interbedded with carbonate-cemented sandstones with *Nereites* ichnofacies (Gierlowski-Kordesch and Ernst, 1987; Ernst and Schlüter, 1989; Ernst and Zander, 1993; Nicholas et al., 2006). The overlying Paleogene sediments were subdivided between the Kivinje Fm. (Paleocene–early Eocene), Masoko Fm. (middle Eocene) and Pande Fm. (late Eocene–early Oligocene) (Nicholas et al., 2006). Cenomanian–Coniacian sediments, with one or more unconformities, were proposed to separate the Nangurukuru Fm. from the underlying Aptian–Albian Kingongo Marls (Nicholas et al., 2006; Jiménez Berrocoso et al., 2010) (Fig. 1b).

TDP drilling in 2007 revealed that the Upper Cretaceous sediments underlying the Nangurukuru Fm. in Lindi were more widely distributed and stratigraphically expanded than had previously been observed (Jiménez Berrocoso et al., 2010). In addition to coring lower–upper Campanian sediments (TDP Site 23) that were assigned to the Nangurukuru Fm., upper Albian–Coniacian sections were also described (Jiménez Berrocoso et al., 2010) (Fig. 1b). Planktonic foraminiferal biostratigraphy indicated at least two unconformities separating (1) the *Planomalina buxtorfi* Zone (upper Albian) from the overlying *Thalmanninella globotruncanoides* Zone (lower–middle Cenomanian, previously identified as the *Rotalipora cushmani* Zone in Jiménez Berrocoso et al., 2010) in TDP Site 24, and (2) the *R. cushmani* Zone (middle–upper Cenomanian) from the *Whiteinella archaeocretacea* Zone (lower Turonian) in TDP Sites 24 and 26. Calcareous nannofossil biostratigraphy, however, suggested a complete Albian–Cenomanian boundary interval in TDP Site 24, and a major condensation of the subzones UC3c–UC5c, coincident with the postulated unconformity inferred from planktonic foraminifera between the middle–upper Cenomanian and the lower Turonian in TDP Sites 24 and 26.

From the sediments drilled in 2008, the Paleocene section cored at TDP Site 27 is included in the Kivinje Fm. of Nicholas et al. (2006)

(Fig. 1b). The Campanian recovered at TDP Sites 28, 32 and 35 represents part of the Nangurukuru Fm. (Nicholas et al., 2006), whereas the Cenomanian (TDP Site 33) and the thick Turonian (TDP Sites 29–31 and 34) sections are assigned to the separate stratigraphic unit underlying the Nangurukuru Fm. (Nicholas et al., 2006; Jiménez Berrocoso et al., 2010) (Fig. 1b) that will be formally defined elsewhere.

3. Methods

The methods employed here are similar to those described in more detail in Jiménez Berrocoso et al. (2010). The planktonic foraminiferal biozonation scheme used is based on integration of the standard tropical/subtropical schemes of Robaszynski and Caron (1995) (Mediterranean region), Sliter (1989) (eastern Pacific), Huber et al. (2008) (western Atlantic) and Petrizzo et al. (2011) (Tanzania), which were established for the families Globotruncanidae and Heterohelicidae. Absolute ages assigned to the biozones and secondary datum events, and their reference sources, are shown in Table 1 (Supplementary material). The nannofossil biozonations used here are the NP scheme of Martini (1971) for the Paleocene (TDP Site 27) and the global UC scheme of Burnett et al. (1998) for the Cretaceous (TDP Sites 28–35). Depths for placement of calcareous nannofossils biozones are shown in Table 2 (Supplementary material). High-resolution work on the nannofossils is ongoing for all sites, and a full biostratigraphic report will be published at a later date.

The $\delta^{13}C_{carb}$ and $\delta^{18}O_{carb}$ of bulk carbonate samples were measured at a resolution of ~1 sample/core. The $\%CaCO_3$, $\%C_{org}$ and $\delta^{13}C_{org}$ (carbon isotopic ratio of bulk organic matter) were measured on about half of these samples (that is, at an average resolution of ~1 sample every other core). For most samples, bulk material was ground using an agate mortar and pestle. This powder (or drilled powders in some samples) was used for bulk carbonate isotope measurements using a Kiel III carbonate device interfaced with a Thermo Finnegan Delta Plus isotope ratio mass spectrometer. Samples for $\delta^{13}C_{org}$ were first decarbonated and percent carbonate was calculated from the weight lost. Approximately 5 mg of this decarbonated powder was loaded into tin capsules and analyzed using a Carlo Erba NA 1500 Elemental Analyzer connected through a Finnegan MAT ConFlo III to a Delta Plus XL isotope ratio mass spectrometer. The $\%C_{org}$ was calculated from the amount of CO_2 generated during combustion corrected to sample weight before decarbonation. Error in weight percent is estimated at ~10% of the reported value, based on replicate analyses. Analytical precision (1 standard deviation, s.d.) of the bulk carbonate isotopic analyses is estimated at <0.03‰ and <0.06‰ for carbon and oxygen, respectively, and of bulk organic carbon isotopes at <0.1‰ based on repeated analysis of NBS-19 carbonate and acetanilide organic standards. All isotopic results are expressed in the standard δ-notation relative to the Vienna PDB standard.

4. Results

4.1. TDP Site 27

TDP Site 27 was drilled on top of Kimamba Hill (UTM 37L 574233, 8892237) (Fig. 1 of Supplementary material), which represents a fault-bounded topographic high, interpreted as the surface expression of a deeper-seated flower structure (Nicholas et al., 2007). The site was placed 100 m southeast of a laterite quarry off the Hotelitatu-Lindi road, a few hundred meters north of the Ukuli River bridge. The main objective was to recover the Cretaceous–Paleogene (K–Pg) boundary interval, which previously had been unsuccessfully attempted at TDP Sites 10 and 19 (Kilwa) (Nicholas et al., 2006), and 5 and 25 (Lindi) (Pearson et al., 2004; Jiménez Berrocoso et al., 2010). Surveys in the area had found Paleocene limestones in the upper part of Kimamba Hill and upper Maastrichtian mudstones in the banks of the Ukuli River (Kent et al., 1971; Nicholas et al., 2006). Placing the rig on top of Kimamba Hill was expected to enable recovery of the K–Pg boundary interval some distance below the surface. However, at TDP Site 27, core recovery was poor in the upper portion of the borehole and drilling terminated in unconsolidated sands at 18.40 m, with Paleocene, but no Cretaceous, sediment cored.

4.1.1. Lithostratigraphy

The upper 5.7 m of this site (cores TDP27/1–4) show grayish orange, weathered limestones, with macrofossil fragments (e.g., bivalves and corals) that become more abundant down core (Figs. 2 and 3a). Cores TDP27/5–6 (from 8 to 10 m) yield brecciated limestones, with angular clasts (up to 10 cm across) and occasional carbonaceous smears in a dark orange, lithified, sandy matrix. A 0.8-cm-thick, soft, olive gray claystone layer (Figs. 2 and 3b) overlies 2.8-cm-thick, gray, calcareous sandstone beds (from 10.8 to 13.6 m) that include fossiliferous (e.g., gastropods and corals) limestone clasts (cores TDP27/7–9) (Figs. 2 and 3c). Claystone interbeds occur within this interval. From 14 m to the bottom of the hole (cores TDP27/10–14), the dominant lithologies are olive gray, bioturbated, sandy limestones (Figs. 2 and 3d) that show

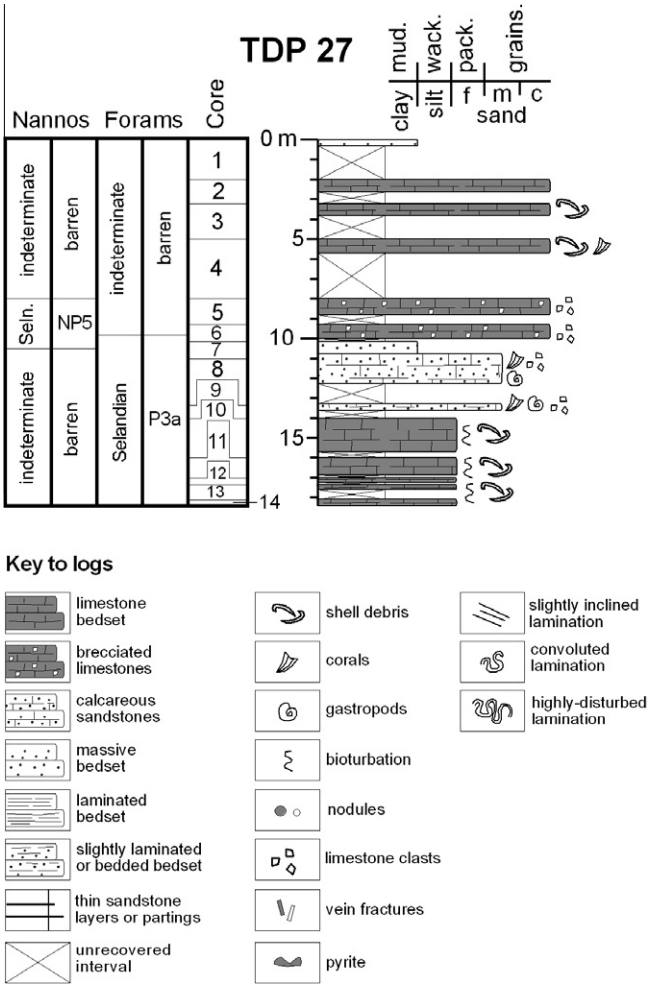

Fig. 2. Integrated lithostratigraphy, planktonic foraminiferal and calcareous nannofossil biostratigraphy, and chemostratigraphy of TDP Site 27. Lower limit of weathering is below core 14.

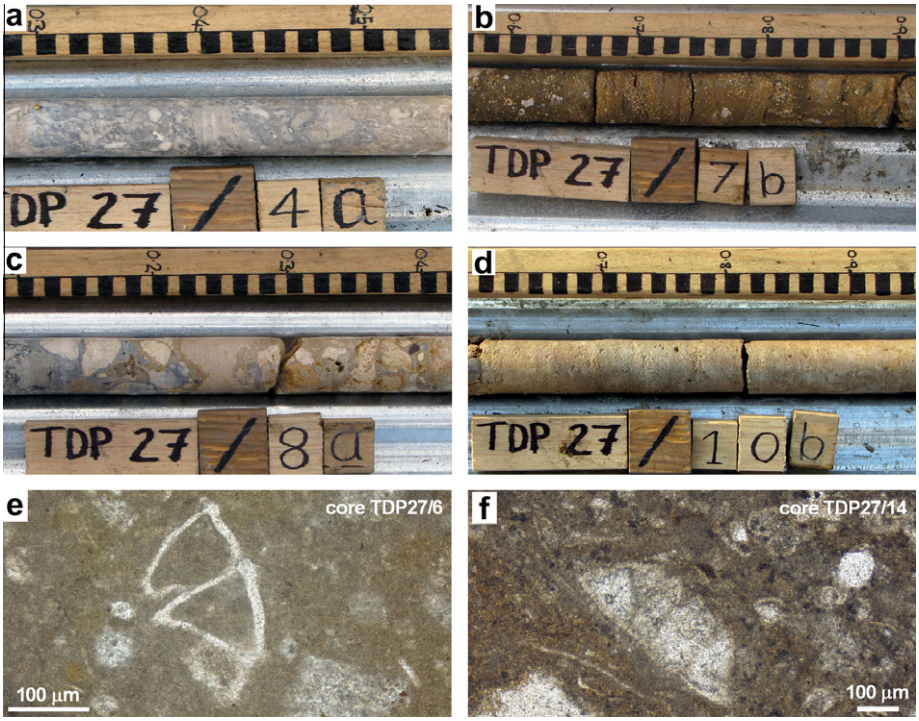

Fig. 3. Photographs of TDP Site 27 (middle Paleocene). (a) Limestone with abundant bioclasts (corals and bivalves). (b) Soft claystone with abundant, well-preserved planktonic foraminifera. (c) Fossiliferous sandstone with common limestone clasts. (d) Bioturbated, sandy limestone at bottom hole. (e and f) Thin-section views of limestones with, respectively, *Morozovella angulata* and *M. pasionensis*. Ruler divisions in core photos are in cm.

dispersed shell debris and become finer-grained and more clay-rich towards the bottom.

Highly bioclastic packstone–grainstone fabrics are visible in thin-sections of cores TDP27/1 and 6. The bioclasts correspond to coralline encrusting red algae, dasyclad green algae, recrystallised corals, Paleocene peyssonellid encrusting algae, and benthic and planktonic foraminifera (Fig. 3e), together with quartz grains. The presence of dasyclad green algae suggests a depositional setting of <30 m water depth. Thin-sections of cores TDP27/11, 13 and 14 show wackestone–packstone textures and a lower percentage of bioclasts, which mainly consist of benthic and planktonic foraminifera (Fig. 3f) and sporadic occurrences of ostracods and red algae. This assemblage may indicate a slightly deeper depositional setting.

4.1.2. Foraminiferal biostratigraphy

No sieved residues were studied from cores TDP27/1–5 (Fig. 2), but the two samples from core TDP27/6 contain rare planktonic and common benthic foraminifera. Foraminiferal tests are commonly infilled with calcite and the external walls show good preservation only occasionally. Benthic assemblages in this core include possible *Nuttalides* sp., *Lenticulina* sp., *Nodosarina* sp., *Cibicidoides* sp., *Anomalinoides* sp., *Dentalinoides* sp., *Neoflabellina* sp. and *Gyroidinoides* sp., which all suggest a shallow-water, near-shore depositional setting, consistent with the interpretation of thin-sections. Planktonic assemblages variably contain *Morozovella angulata*, *M. velascoensis*, *M. pasionensis*, *M. apanthesma*, *Subbotina cancellata*, *S. triloculinoides*, *Parasubbotina varianta* and *Globanomalina chapmani* and indicate a middle Paleocene (Selandian) age, within Zone P3a (Fig. 2).

Planktonic foraminiferal preservation and abundance are particularly good in a sample collected from core TDP27/7 (10.3 m depth) (Figs. 2 and 3b). Here, planktonic foraminifera outnumber benthic foraminifera, and shell preservation is excellent, despite infilling with calcite. Species recorded include *Morozovella angulata*, *M. praeangulata*, *Subbotina cancellata*, *S. triangularis*, *S. triloculinoides*, *Parasubbotina varianta*, *P. pseudobulloides*, *Praemurica uncinata*, *Pr. inconstans*, *Pr. pseudoinconstans*, *Globanomalina chapmani* and *G. ehrenbergi*. The lack of *M. velascoensis*-group morozovellids and the presence of *Pr. uncinata* and other species of *Praemurica* suggest a middle Paleocene age for this sample, within Zone P3a (Fig. 2). Below this sample, cores TDP27/11–14 show an assemblage with poorly preserved and rare planktonic foraminifera (*M. angulata*, *P. varianta, S. triloculinoides*, *Pr. uncinata* and *S. cancellata*), attributed to Zone P3a.

Thin-sections studied from this site show only a few planktonic foraminifera. Distinctive Paleocene species include *Morozovella angulata, M. velascoensis*-group morozovellids (*M. pasionensis* and *M. occlusa*) and compressed *Globanomalina* sp. These species occur in various combinations in cores TDP27/1, 6, 11, 13 and 14 (Fig. 3e and f). Interestingly, however, all thin-sections from these limestones appear to contain morphologies diagnostic of Zones P3b–P4, whereas the washed residues suggest the slightly older Zone P3a (Fig. 2). A better preservation of marker species in washed residues, and/or slight downhole contamination, might explain this age offset.

4.1.3. Calcareous nannofossil biostratigraphy

Out of the 17 samples studied, only six contained calcareous nannofossils. Cores TDP27/5–7 show common to abundant and exceptionally well-preserved specimens, with diverse assemblages yielding higher species richness (~90 species in total) than tabulated for Paleogene in the global compilation of Bown et al. (2004). The quality of preservation is evident from the presence of abundant small coccoliths (*Prinsius* and *Toweius*) and conspicuous small and fragile taxa (holococcoliths and *Calciosolenia*). The assemblages are dominated by *Prinsius, Toweius, Coccolithus, Neochiastozygus, Ericsonia, Umbilicosphaera jordanii* and *Zeugrhabdotus sigmoides*. *Ellipsolithus* coccoliths are also frequent to common and diverse. The presence of *Pontosphaera* spp. is

particularly notable, since the family and genus has not previously been found in sediments older than latest Paleocene (Zone NP9) (e.g., Bybell and Self-Trail, 1995). Most samples also contain rare reworked nannofossils of the middle to Late Cretaceous (e.g., *Micula, Eiffellithus, Watznaueria* and *Retecapsa*).

The presence of *Ellipsolithus macellus* and the absence of *Heliolithus kleinpellii* or discoasters in the samples from cores TDP27/5–7 indicate an age equivalent to Zones NP4 or NP5. Although *Fasciculithus* spp. are rare, the presence of forms that resemble *F. tympaniformis* suggests these cores fall within the

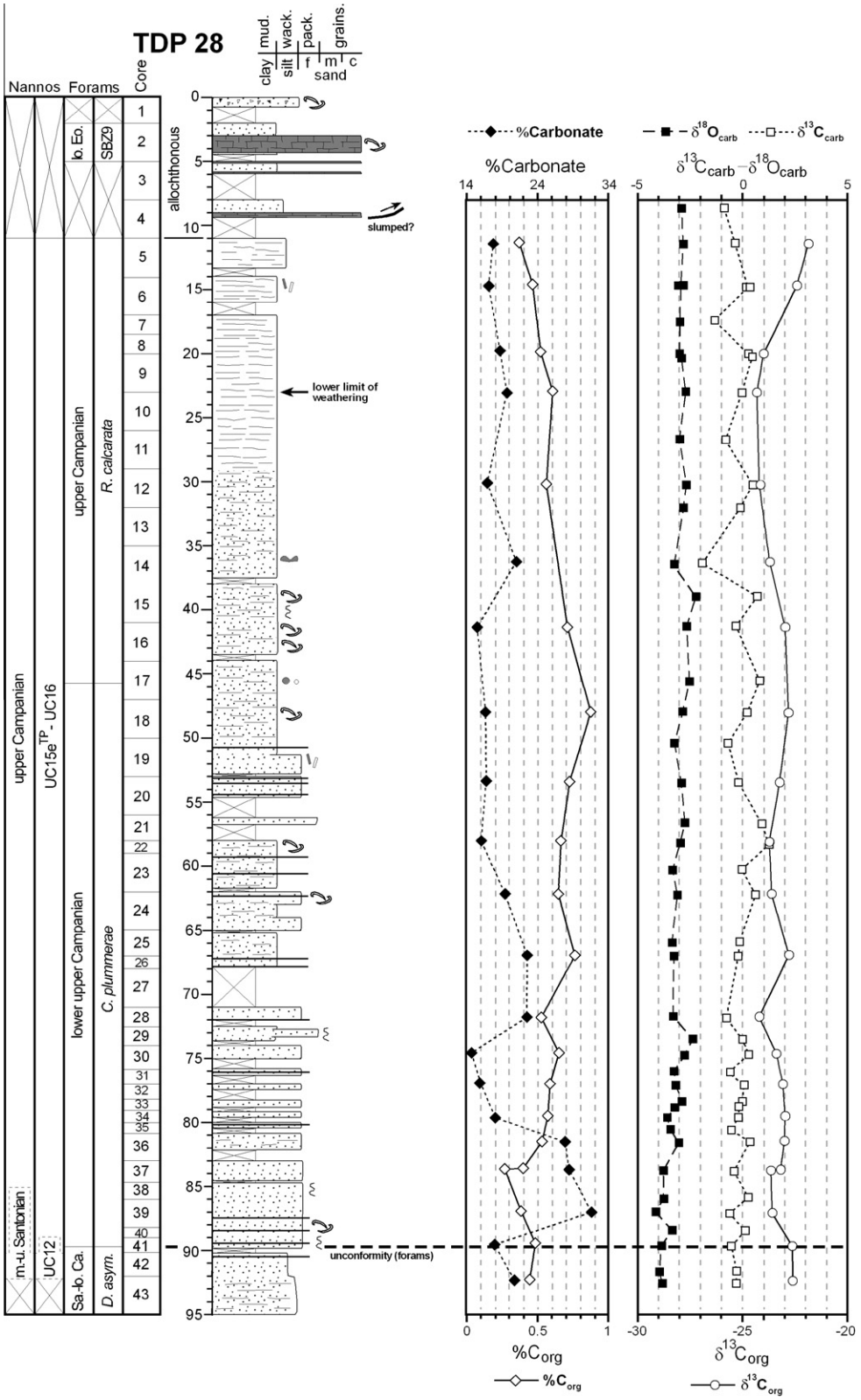

Fig. 4. Integrated lithostratigraphy, planktonic foraminiferal and calcareous nannofossil biostratigraphy, and chemostratigraphy of TDP Site 28. Lower limit of weathering indicated in core 9. Dashed lines in calcareous nannofossil columns indicate that placement of zonal boundaries is not considered final. Symbols as given in Fig. 2.

Selandian Zone NP5 (Fig. 2). This is further supported by the presence of *Sphenolithus, Toweius eminens* and *Neochiastozygus perfectus* (e.g., Varol, 1998; Bernaola et al., 2009).

4.2. TDP Site 28

TDP Site 28 was drilled 20 m south of the main road, 5 km southwest of Lindi (UTM 37L 574233, 8892237) (Fig. 2 of Supplementary material). The main goals were to drill the lower to upper Campanian and try to recover foraminifera with better preservation than in TDP Site 23, which had yielded sediments of this age with occasional glassy preservation, just 1 km to the north–northwest (Jiménez Berrocoso et al., 2010). The site was drilled to 95 m, with low to moderate recovery from the surface to 17 m, and good recovery from 17 m to the bottom of the hole. Drilling was terminated in Santonian sediments from the *Dicarinella asymetrica* Zone.

4.2.1. Lithostratigraphy and bulk sediment composition

Lithologies from the surface to the middle part of core TDP28/4 (9.27 m) are composed of dark yellow brown, weathered, silty claystones, with intervals of yellow brown, well-lithified, massive, bioclastic grainstones (Figs. 4 and 5a). These grainstones were cored just below the surface of a disused road bed and present sharp, angular contacts with the surrounding lithologies (Fig. 5a), which indicate mechanical and not depositional surfaces. Also, this interval is not older than Eocene (Section 4.2.2), whereas all recovered sediments underlying core TDP28/4 belong to the Campanian (Fig. 4). Thus, we consider the top portion of this site to represent an allochthonous block (Fig. 4) related to either road rubble or to a large slump system off the west side of Kitulo Hill (Pearson et al., 2004).

From 11 m (core TDP28/5) to the bottom of the hole, the main lithologies are olive gray to olive black siltstones and silty claystones (Figs. 4 and 5b). Fine lamination is commonly observed throughout the hole, but especially from cores TDP28/5–11 (11–29 m). Calcite vein fractures (cores TDP28/6 and 19), cm- to mm-sized, fine sand nodules (core TDP28/17), small bioturbation burrows (cores TDP28/15, 29, 38 and 41) and shell debris (e.g., inoceramids) (cores TDP28/15, 16, 18, 22, 24 and 40) are occasionally visible. Light gray, sandy partings are relatively frequent in the middle and lower part of the hole (50.88–90.50 m) (Figs. 4 and 5b).

The $\%CaCO_3$ in this site ranges from 14.4% to 31.3% (average = 20.1 ± 4.90%, 1 s.d.) and the $\%C_{org}$ from 0.3% to 0.9% (average = 0.56 ± 0.15‰, 1 s.d.). The $\%CaCO_3$ is higher in three samples between 81 and 87 m (Fig. 4), compared to the rest of the samples. However, no clear vertical patterns are observed in the $\%CaCO_3$ and $\%C_{org}$ profiles (Fig. 4).

4.2.2. Foraminiferal biostratigraphy

A thin-section at 3.21 m, from a well-lithified grainstone in core TDP28/2 (Fig. 4), contains an uppermost Paleocene–lower Eocene larger foraminiferal assemblage composed of discocyclinids, *Nummulites*, large *Assilina* and *Glomalveolina*, as well as coralline algae. The presence of one specimen resembling *Nummulites involutus* could be indicative of the lower Eocene Zone SBZ9 (*sensu* Serra-Kiel et al., 1998).

Planktonic foraminifera from cores TDP28/5–43 generally occur in greater abundance than benthic foraminifera. Preservation is moderate to good, with sporadic occurrences of glassy specimens. Cores TDP28/5–17 (11.63–45.72 m) are assigned to the upper Campanian *Radotruncana calcarata* Zone (Fig. 4), based on the presence of the nominate species. The underlying interval (from 45.72 to 89.85 m, cores TDP28/17–41) is diagnostic of the upper part of the *Contusotruncana plummerae* Zone (replacing the former *Globotruncana ventricosa* Zone: Petrizzo et al., 2011) and indicates the existence of the lower upper Campanian, based on both the co-occurrence of *C. plummerae, G. ventricosa* and *R. subspinosa* and the absence of *R. calcarata*. Noteworthy is the rarity of *Globotruncanita elevata* in this interval. An unconformity that spans at least the thickness of the *G. elevata* Zone is detected in core TDP28/41 (Fig. 4). The underlying sediments (cores TDP28/42–43) are assigned to the *Dicarinella asymetrica* Zone (Santonian–lower Campanian), based on the presence of the nominate species. The occurrence of *Sigalia carpathica* from 90.27 to 92.81 m (cores TDP28/42–43) confirms a Santonian–lower Campanian age for the bottom of the hole.

4.2.3. Calcareous nannofossil biostratigraphy

Nannofossil abundance in the samples studied from TDP Site 28 is variable and preservation is generally moderate to good. These samples indicate the existence of the upper Campanian Zones UC15e^{TP}–UC16 from 11.18 to 90.17 m (cores TDP28/5–41) and the middle–upper Santonian Zone UC12 from 90.17 to 92 m (cores TDP28/41–42; Fig. 4).

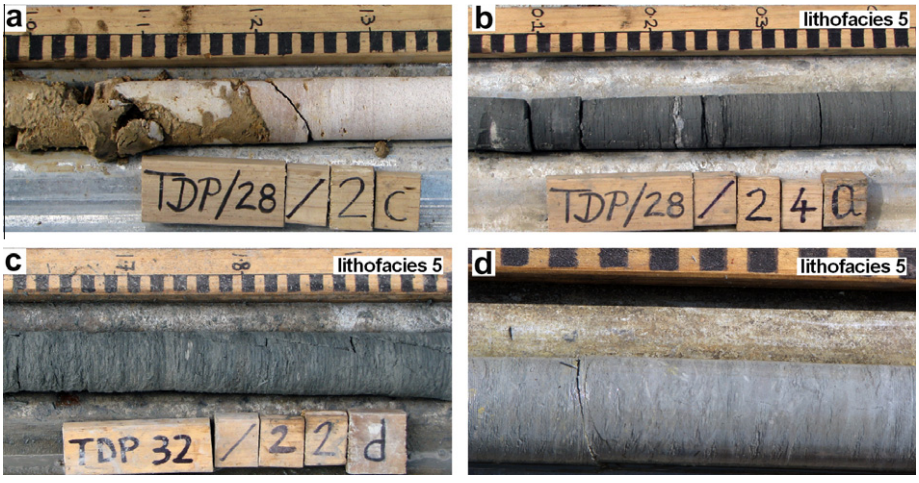

Fig. 5. Core photographs of TDP Sites 28, 32 and 35 (Santonian–upper Campanian), with representative views of the inferred lithofacies 5. (a) Sharp, angular contact between weathered claystone and limestone. (b) Slightly laminated siltstone with light gray, sandy partings at ~7 and ~22 cm. (c) Monotonous claystone with slight lamination. (d) Siltstone with abundant bioturbation burrows in core TDP35/10. Ruler divisions are in cm.

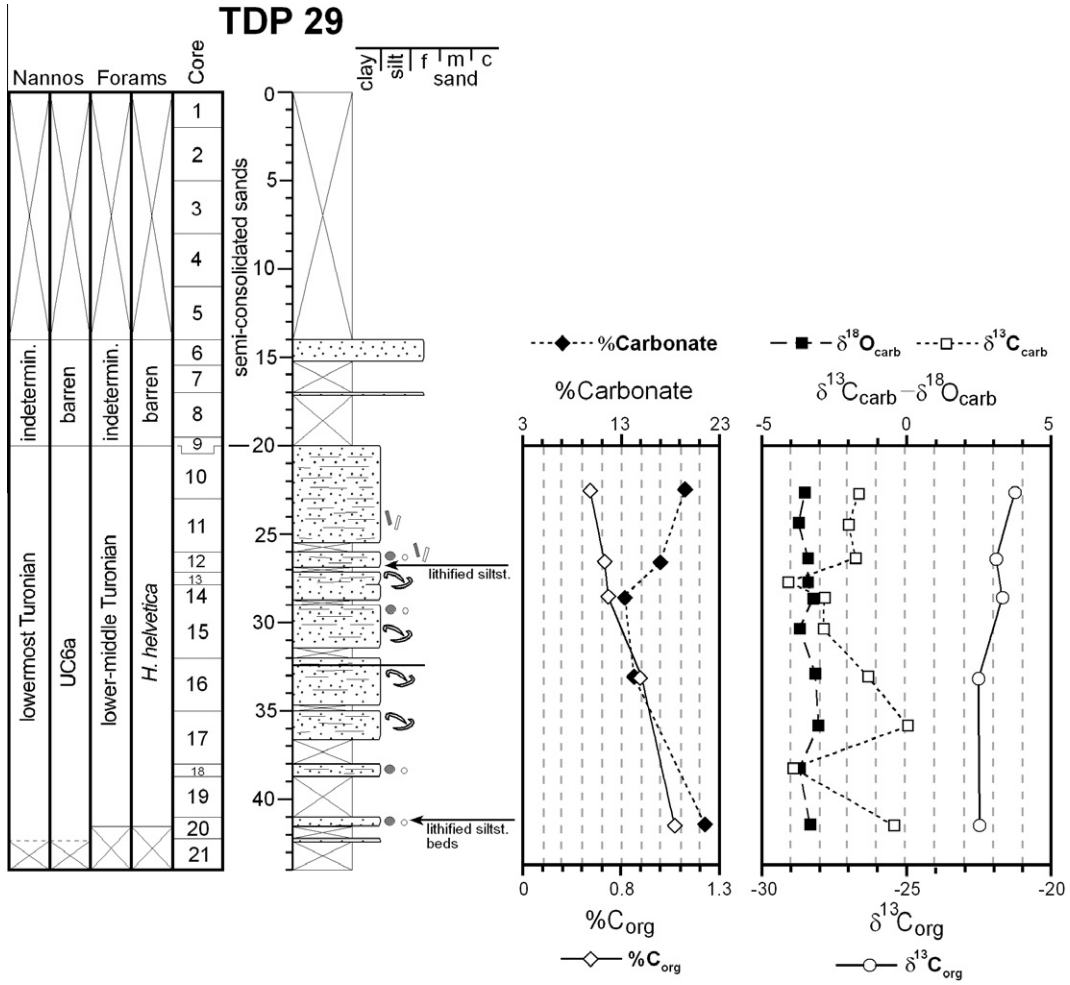

Fig. 6. Integrated lithostratigraphy, planktonic foraminiferal and calcareous nannofossil biostratigraphy, and chemostratigraphy of TDP Site 29. Lower limit of weathering is below core 21. Dashed lines in calcareous nannofossil columns indicate that placement of zonal boundaries is not considered final. Symbols as given in Fig. 2.

4.2.4. Chemostratigraphy

The $\delta^{13}C_{org}$ for TDP Site 28 ranges from −24.5‰ to −21.7‰ (average = −23.2 ± 0.75‰, 1 s.d.). There is no obvious vertical trend in this profile, but fluctuations of 2–3‰ spanning 5–30 m are present (Fig. 4). Parallel trends are not seen in the $\delta^{13}C_{carb}$ profile and neither $\%CaCO_3$ nor $\%C_{org}$ correlate with the $\delta^{13}C_{org}$ or $\delta^{13}C_{carb}$ curves. Altogether, this suggests that the $\delta^{13}C_{org}$ fluctuations do not represent regional or global shifts among carbon reservoirs, but likely local changes in the relative proportions of terrestrial and marine organic matter. The $\delta^{13}C_{carb}$ ranges from −2.9‰ to 1.3‰ (average = −0.10 ± 0.63‰, 1 s.d.) and the $\delta^{18}O_{carb}$ from −4.3‰ to −2.2‰ (average = −3.22 ± 0.48‰, 1 s.d.). Both values are relatively constant through most of the section (Fig. 4), but there is an increase in $\delta^{18}O_{carb}$ of ~1‰ from the bottom of the hole up to 73.68 m. This shift may represent cooling from the Santonian into the early late Campanian. In addition, there are multiple, single-point, negative excursions in the record of $\delta^{18}O_{carb}$ and $\delta^{13}C_{carb}$ that often are present in the same samples and likely reflect the presence of diagenetically altered carbonate.

4.3. TDP Site 29

TDP Site 29 was drilled 0.6 km east of the main road, 12.5 km to the southwest of Lindi (UTM 37L 568268, 8886723) (Fig. 2 of Supplementary material). The site is 460 m east of TDP Site 22, which drilled a lower–middle Turonian sequence (*Whiteinella archaeocretacea* to *Helvetoglobotruncana helvetica* Zones) from 11 to 134 m (Jiménez Berrocoso et al., 2010). Goals for this site were to drill lower Turonian sediments and recover the Cenomanian–Turonian boundary interval. The site was drilled to 44 m, with no recovery from the surface to 14 m, good recovery from 14 to 37.64 m, and low recovery from 37.64 m to the bottom of the hole (Fig. 6). The upper 20 m (cores TDP29/1–9) yielded semi-consolidated sands that were barren of microfossils. This interval may correlate with the loose-sand package cored in the upper 11 m of TDP Site 22 (Jiménez Berrocoso et al., 2010). Drilling was terminated in lower–middle Turonian sediments at only 44 m depth due to caving of sands and binding of the drill-pipe at the bottom of the hole.

4.3.1. Lithostratigraphy and bulk sediment composition

The principal lithologies from 20 m (core TDP29/10) to the bottom of the hole are olive gray to olive black, massive to slightly-bedded, silty claystones (Fig. 6). A few intervals (mm to cm thick) with waxy, possibly organic-rich, darker claystones occur in cores TDP29/16 and 18. Sub-horizontal and cross-cutting sulfate–carbonate veins are only locally observed, as well as yellowish brown, mm- to cm-sized sand nodules. Cores TDP29/12 and 20 present a light gray, cm-thick, well-lithified, carbonate-cemented siltstone layer (Figs. 6, 7a and b), with sharp top and basal contacts. Bivalve shell debris is sporadically present in cores TDP29/13 and 15–17.

No apparent relationship is observed between the $\%CaCO_3$ and $\%C_{org}$ in the analyzed bulk samples of TDP Site 29 (Fig. 6). The carbonate content ranges from 13.6% to 21.9% (17.37 ± 3.47%, 1

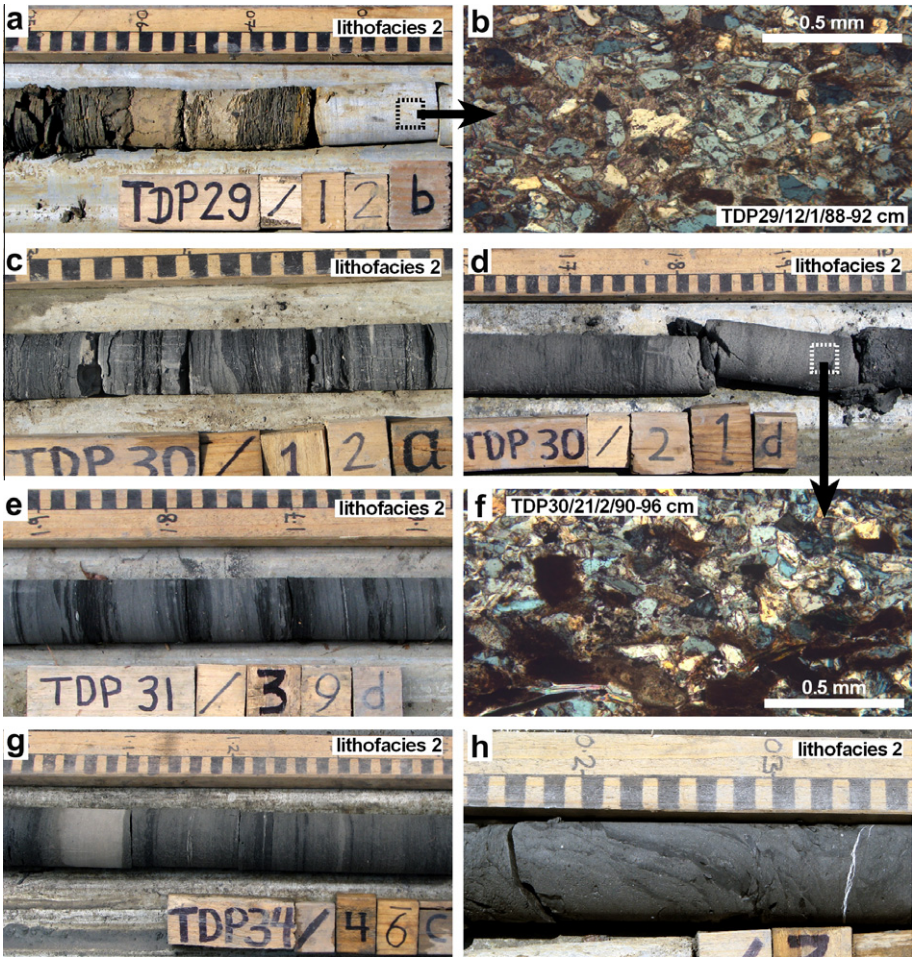

Fig. 7. Photographs of TDP Sites 29, 30, 31 and 34 (lower Turonian–Coniacian), with representative views of lithofacies 2. (a) Dark gray claystones and light gray, well-lithified siltstone; black, dashed-line rectangle represents position of thin-section in (b). (b) Thin-section view of light gray siltstone in (a); the abundant angular to sub-angular grains are monocrystalline quartz cemented by calcite. (c) Interbedded, olive black claystones and sandy siltstones; note sharp, erosive contact between siltstone (medium gray) and claystone (dark gray) layer towards middle. (d) Olive black, well-lithified siltstone layer (broken interval) and massive claystones; white, dashed-line rectangle represents position of thin-section in (f). (e) Interbedded dark gray siltstone and organic-rich claystone intervals. (f) Thin-section view of olive black siltstone in (d), in which majority of grains (monocrystalline quartz) are cemented by quartz. (g) Well-lithified siltstone bed (left side) and interbedded, dark gray siltstones and claystones. (h) Highly disturbed lamination in core TDP34/37.

s.d.) and the organic carbon from 0.6% to 1.1% (0.82 ± 0.18%, 1 s.d.). Carbonate content is relatively low in the upper 30 m of the section and higher in the lower 14 m. Organic carbon content seems to increase progressively with depth.

4.3.2. Foraminiferal biostratigraphy

Foraminifera were not recovered in cores TDP29/6–9 of this site (Fig. 6). In the underlying sediments (cores TDP29/10–20), planktonic foraminifera are rare to common and preservation ranges from good to excellent in most samples. These sediments are assigned to the lower–middle Turonian *Helvetoglobotruncana helvetica* Zone (Fig. 6) due to the presence of the nominate taxon and its co-occurrence with *H. praehelvetica*, *Dicarinella hagni*, *D. paraconcavata* and several species of *Whiteinella* (e.g., *W. aprica*, *W. brittonensis*, *W. archaeocretacea*).

Benthic foraminifera are more common than planktonic foraminifera in most samples from cores TDP29/10–21 and are mostly composed of broken, agglutinated, tubular and branching rhabdamminids, and agglutinated planispiral and low trochospiral forms (Haplophragmoididae and Trochamminidae). The benthic assemblages also include *Ammodiscus* sp., *Glomospira* sp., *Dorothia oxycona*, *Dentalina* sp., *Lenticulina* spp., *Marginulina* sp., *Praebulimina* sp., *Gavelinella* sp., *Berthelina berthelini*, *Lingulogavelinella convexa*, *Eponides* sp., *Gyroidinoides* spp., *Epistomina* spp. and *Pseudosigmoilina* spp. Abundance and diversity of benthic species vary strongly between the samples studied, probably reflecting a combination of fluctuating oxygen in bottom waters, food supply and fluxes of terrigenous material to the seafloor.

4.3.3. Calcareous nannofossil biostratigraphy

Samples studied from cores TDP29/6–9 were barren of nannofossils. The underlying sediments (cores TPD29/10–21) provide calcareous nannofossil assemblages that are assigned to Zone UC6a (lowermost Turonian) (Fig. 6) based on the absence of *Helenea chiastia* and *Eprolithus moratus*. This biostratigraphic interpretation, however, does not agree with the observed planktonic foraminiferal biostratigraphy from the same cores (lower–middle Turonian *Helvetoglobotruncana helvetica* Zone). Although well preserved, a low to very low abundance of calcareous nannofossils in these cores might explain this disagreement. A higher-resolution study is in progress to resolve this biostratigraphic discrepancy.

4.3.4. Chemostratigraphy

Only a few bulk samples were analyzed from TDP Site 29. The $\delta^{13}C_{org}$ values range between −22.5‰ and −21.2‰ (average = −21.9 ± 0.55‰ 1 s.d.) and show no major change through

the section cored (Fig. 6). The $\delta^{13}C_{carb}$ values range from −4.2‰ to 0‰ (average = −2.1 ± 1.4‰, 1 s.d.) and they follow no overall vertical trend, but vary greatly between points, especially in the samples below 30.54 m. The $\delta^{18}O_{carb}$ values range from −3.8‰ to −3.1‰ (average = −3.5 ± 0.24‰, 1 s.d.) and, similar to other Turonian TDP sites, are relatively consistent and low (Fig. 6).

4.4. TDP Site 30

TDP Site 30 was drilled 200 m west-northwest of the main road, 13.4 km to the southwest of Lindi (UTM 37L 567556, 8886974) (Fig. 2 of Supplementary material). The main goal was to drill the lower Turonian and the Cenomanian–Turonian boundary interval. The site was positioned 300 m and 750 m to the west of TDP Sites 22 and 29, respectively, and at a lower elevation than either of them, in an effort to penetrate below the lower–middle Turonian sediments (*Whiteinella archaeocretacea* to *Helvetoglobotruncana helvetica* Zones) recovered at these two sites (Jiménez Berrocoso et al., 2010). TDP Site 30 was drilled to 113 m, with good recovery throughout. Similar to TDP Sites 22 and 29, the upper part of TDP Site 30 showed a 4.65-m-thick interval of unconsolidated sands that were barren of fossils (Fig. 8). Drilling was terminated at the maximum penetration depth achievable by the rig, but no Cenomanian strata were cored.

4.4.1. Lithostratigraphy and bulk sediment composition

The main lithologies from 4.65 m (core TDP30/3) to the bottom of the hole are mm- to cm-thick, interbedded, olive black claystones and sandy siltstones (Figs. 7c and 8), with common occurrence of finely-laminated intervals throughout. Olive black, well-lithified, quartz-cemented siltstone layers are observed at the bottom of cores TDP30/21 and 42 (Fig. 7d and f), whereas light gray, thin sandstone partings are rare in this hole. Sulfate–carbonate vein fractures are sporadically present, while yellowish brown, mm- to cm-sized sand nodules and small shell debris (e.g., bivalves, inoceramids and gastropods) occur relatively often. Soft-sediment deformation, such as slightly inclined and convoluted laminations, is observed in parts of cores TDP30/16, 19–20, 22–27, 31–34 and 42 (Fig. 8). Also, highly disturbed lamination, as evidence of intense soft-sediment deformation, occurs in parts of cores TDP30/13, 15–19, 20 and 34.

The $\%CaCO_3$ throughout this section ranges from 10.9% to 20.8% (average = 15 ± 2.40%, 1 s.d.) and the $\%C_{org}$ from 0.6% to 1.3% (average = 0.91 ± 0.15%, 1 s.d.). The two parameters are inversely related in cores TDP30/3–17 (Fig. 8), whereas they tend to be correlated from core TDP30/18 to the bottom of the hole. These variations, however, do not correlate to changes in the $\delta^{13}C_{org}$ and $\delta^{13}C_{carb}$ profiles.

4.4.2. Foraminiferal biostratigraphy

Abundant planktonic foraminifera, with moderate to good preservation, are observed in most samples from core TDP30/3 to the bottom of the hole. Some intervals show specimens with glassy shells and others with poor preservation and complete shell infilling. Planktonic foraminifera indicate the lower–middle Turonian *Helvetoglobotruncana helvetica* Zone from 4.80 to 37.53 m (cores TDP30/3–17) (Fig. 8), based on the presence of the nominate taxon together with *Dicarinella hagni*, *Praeglobotruncana* spp., *Whiteinella aprica*, *Marginotruncana paraconcavata* and *M. renzi*. The *W. archaeocretacea* Zone (lower Turonian) is recognized from 37.53 m (core TDP30/17) to the bottom of the hole (Fig. 8) based on the absence of *H. helvetica* and Cenomanian rotaliporids as well as on the presence of *D. hagni* and several species of *Whiteinella*.

Most samples studied from TDP Site 30 show either similar or slightly higher abundance of benthic than planktonic foraminifera. Only a few samples from cores TDP30/8–9 exhibit clear dominance of benthic over planktonic foraminifera, but this situation is related to the elevated presence of agglutinated forms. In other cases (cores TDP30/5–7), slightly higher abundances of planktonic foraminifera are found. Benthic foraminiferal diversity is moderate to low in most samples. The assemblages include *Epistomina* spp., *Lenticulina* spp., *Eponides* sp., *Gyroidinoides* spp., *Lingulogavelinella convexa*, *Pseudosigmoilina* spp., *Nodosaria* sp., *Dorothia oxycona*, *Ammodiscus* sp., *Ramulina* sp., *Praebulimina* sp., haplophragminids, trochamminids and agglutinated tubular forms.

4.4.3. Calcareous nannofossil biostratigraphy

Nannofossil abundances in the samples studied from this site range from low to high, and preservation is generally moderate to good. These samples indicate the lower Turonian Zones UC6b(-7?) from core TDP30/3 to the bottom of the hole (Fig. 8).

4.4.4. Chemostratigraphy

The $\delta^{13}C_{org}$ values for TDP Site 30 range between −23.1‰ and −20.7‰ (average = −21.9 ± 0.65‰, 1 s.d.). In general, they show a stable vertical trend, although a broad minimum is visible in the upper part of the *Whiteinella archaeocretacea* Zone (from −20.7‰ to −23.1‰ between cores TDP30/27–19), followed by a 1.3‰ positive shift across the boundary with the *H. helvetica* Zone (Fig. 8). The $\delta^{13}C_{carb}$ profile exhibits a much higher range of values, from −10.6‰ to 1.3‰ (average = −1.95 ± 2.71‰, 1 s.d.). This high range is imparted by the existence of single-point, negative excursions (Fig. 8). Markedly low $\delta^{18}O_{carb}$ values are observed in a majority of the samples with large, negative $\delta^{13}C_{carb}$ excursions, which suggests these large isotopic excursions have a diagenetic origin. The range of the $\delta^{18}O_{carb}$ is from −8.0‰ to −2.9‰ (average = −3.75 ± 1.13‰, 1 s.d.), but most values are around −3.5‰, which may represent the primary isotopic signal.

4.5. TDP Site 31

TDP Site 31 was drilled 0.5 km east of the main road, 8 km to the southwest of Lindi (UTM 37L 570745, 8891215) (Fig. 2 of Supplementary material). The site is 0.20 km to the northwest of a surface sample containing the upper Turonian foraminiferal marker *Marginotruncana schneegansi*. The main goals were to drill the middle–upper Turonian and correlate this site with the lower–middle Turonian of TDP Sites 22, 29 and 30 (Figs. 6 and 8). The site was drilled to 115 m, with moderate recovery from the surface to 41 m and good recovery between 41 m and the bottom of the hole. Drilling was stopped in the lower Turonian *Whiteinella archaeocretacea* Zone, at the maximum penetration depth of the rig.

4.5.1. Lithostratigraphy and bulk sediment composition

The dominant lithologies from the surface to 28 m are olive brown, olive gray and greenish black claystones and silty claystones, with massive or slightly-laminated fabrics (Fig. 9). Sub-horizontal sulfate–carbonate veins are observed at several levels. The interval from 28 m to the bottom of the hole shows mm- to cm-thick, interbedded, medium to dark gray siltstones, silty claystones and claystones, with common, finely-laminated, possibly organic-rich intervals (Figs. 7e and 9). Two intervals with light gray, well-lithified siltstones and cross-cutting sulfate–carbonate veins are visible in cores TDP31/22 and 24. Light gray, fine-grained sandstone partings are present sporadically from 28 m to the bottom. Yellowish brown, mm- to cm-sized sand nodules occur occasionally through the middle and lower intervals of the hole. Ammonite and inoceramid debris are relatively frequent in the same intervals (Fig. 9). Slightly inclined lamination, indicative of moderate soft-sediment deformation, is present throughout the hole, but is less common than at TDP Site 30.

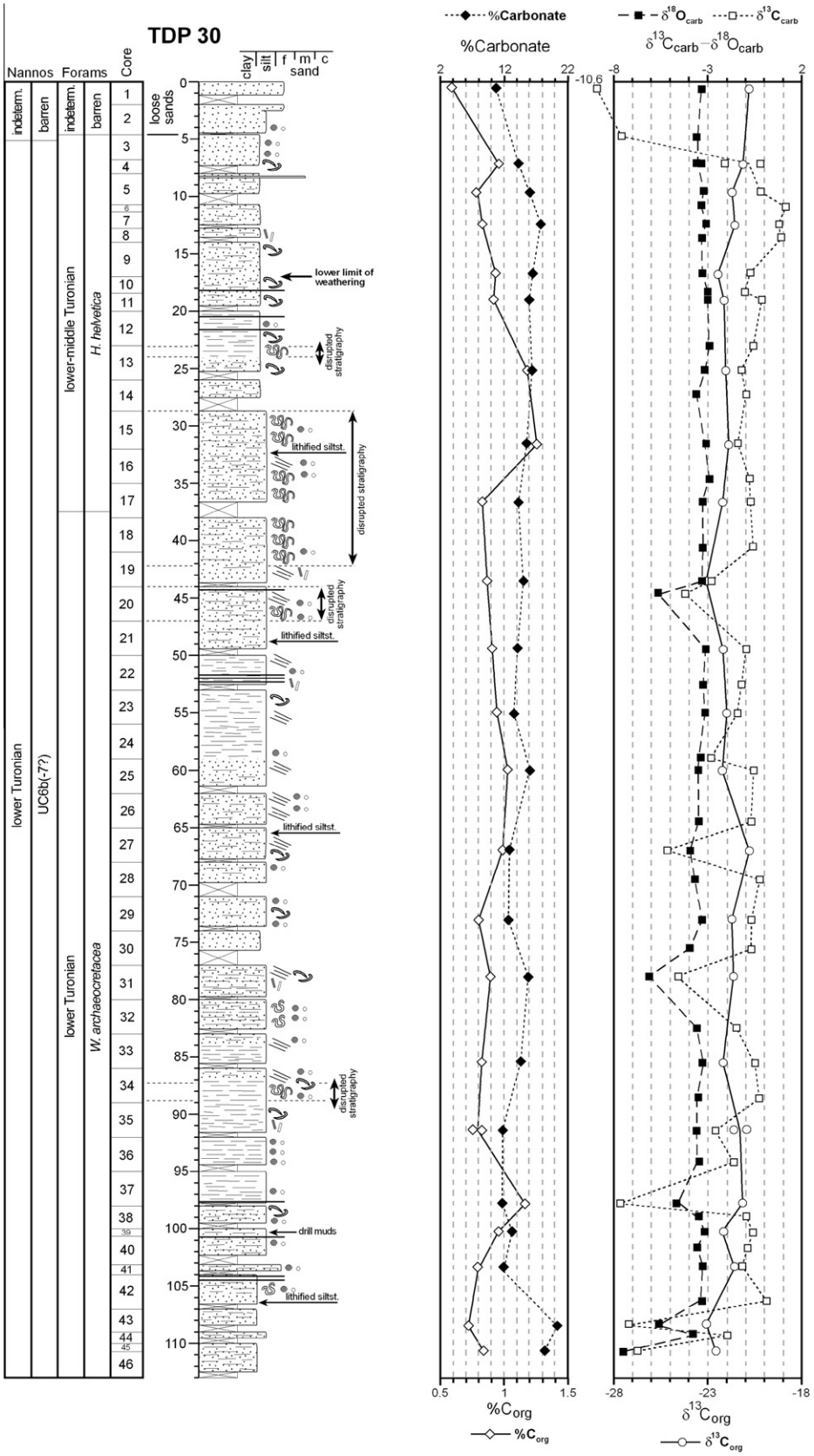

Fig. 8. Integrated lithostratigraphy, planktonic foraminiferal and calcareous nannofossil biostratigraphy, and chemostratigraphy of TDP Site 30. Lower limit of weathering indicated in core 9. Zone UC6b(-7?) indicates that cores 3–47 possibly cover part of Zone UC7. Symbols as given in Fig. 2.

The %$CaCO_3$ and %C_{org} from this site vary inversely throughout the section (Fig. 9), with the former ranging from 3.7% to 37% (average = 13.27 ± 5.30%, 1 s.d.) and the latter from 0.1% to 2.1% (average = 0.88 ± 0.45%, 1 s.d.). Despite this relatively high variability in the values of both parameters, there is no apparent vertical trend in the sediments below 60 m (core TDP31/37–64) (Fig. 9).

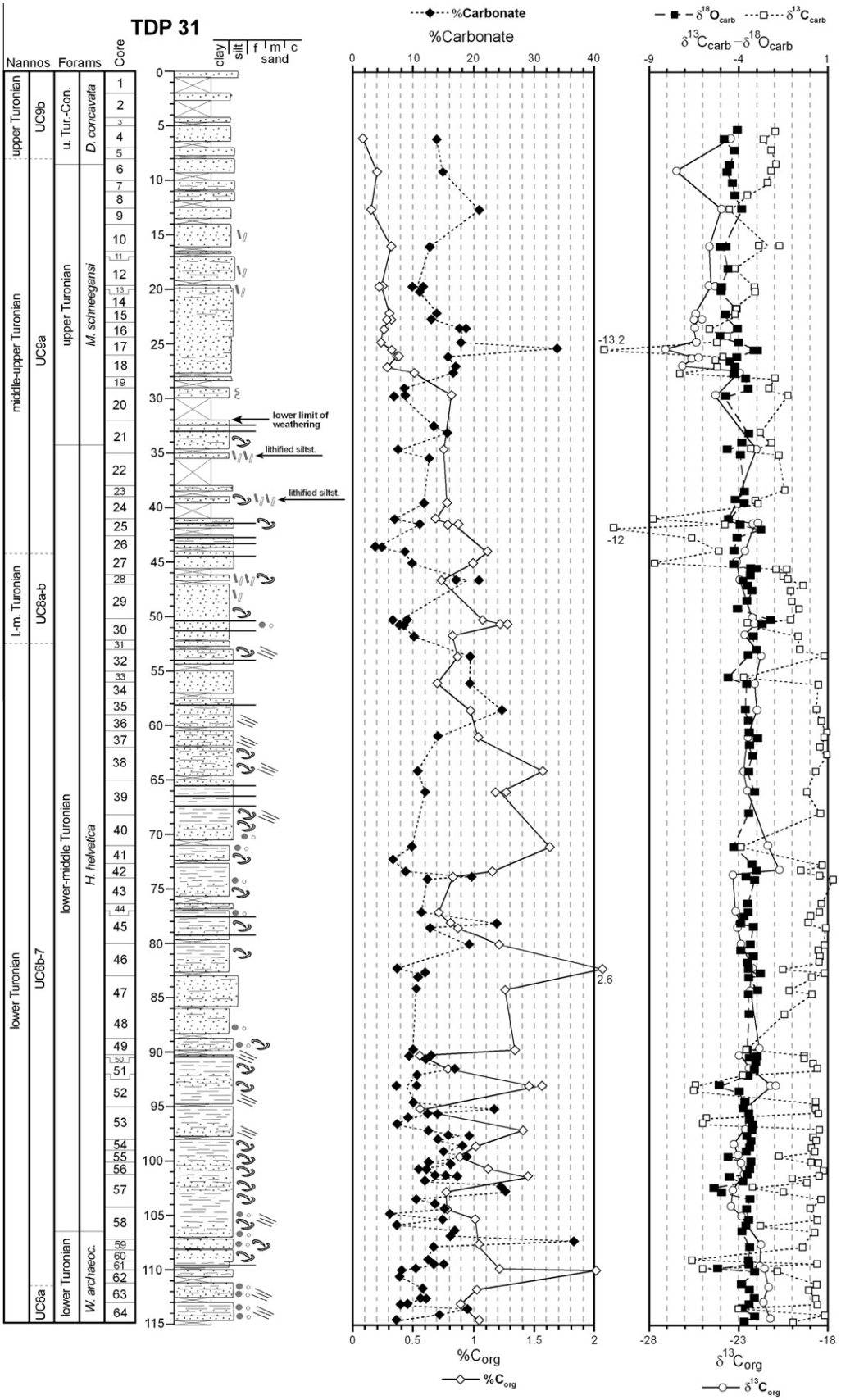

Fig. 9. Integrated lithostratigraphy, planktonic foraminiferal and calcareous nannofossil biostratigraphy, and chemostratigraphy of TDP Site 31. Lower limit of weathering indicated in core 20. Dashed lines indicate that placement of zonal boundaries is not considered final. Symbols as given in Fig. 2.

The $\%C_{org}$ decreases (and the $\%CaCO_3$ increases) from 60 m to the top of the hole, with the sharpest shift near the *Helvetoglobotruncana helvetica–Marginotruncana schneegansi* boundary. This shift correlates with a general decrease in both $\delta^{13}C_{carb}$ and $\delta^{13}C_{org}$ profiles (Section 4.5.4).

4.5.2. Foraminiferal biostratigraphy

All samples from this site yield rare to abundant planktonic foraminifera with moderate to excellent preservation. Relatively high frequency of shell infilling occurs in the upper 25 m (cores TDP31/1–17), whereas glassy shells are common in the lower 90 m (cores TDP31/18–64). Planktonic foraminifera from 0.42 to 8.59 m indicate the upper Turonian–Coniacian *Dicarinella concavata* Zone (cores TDP31/1–6) (Fig. 9), due to the presence of the nominate taxon and the absence of *D. asymetrica*. The upper Turonian *Marginotruncana schneegansi* Zone is identified from 8.59 to 34.11 m (cores TDP31/6–21), based on the absence of *H. helvetica* and *D. concavata* and the presence of *Falsotruncana maslakovae* (Petrizzo, 2001, 2002, 2003). The interval 34.11–106.52 m (cores TDP31/21–58) is assigned to the lower–middle Turonian *Helvetoglobotruncana helvetica* Zone, based on the consistent presence of the nominate taxon with *D. hagni*, *Praeglobotruncana* spp., *Whiteinella aprica*, *M. paraconcavata* and *M. renzi*. Finally, the lower Turonian *W. archaeocretacea* Zone is identified from 106.52 m to the bottom of the hole (Fig. 9), due to the absence of *H. helvetica* and the presence of the nominate taxon, *H. praehelvetica* and *M. paraconcavata*.

Benthic foraminifera in the samples studied average 44% of the total assemblage and range from 14% to 77%. Diversity of benthic species is higher in this site than in TDP Site 30 (Fig. 8). Further, considerably fewer quartz grains are present in the washed residues of this site, compared to TDP Site 30. These observations might suggest either a deeper water-depth or a more distal position, relative to the sediment source, for TDP Site 31 than for TDP Site 30. Most of the samples from the *Whiteinella archaeocretacea* and *Helvetoglobotruncana helvetica* Zones (lower–middle Turonian) of TDP Site 31 show a high relative abundance of agglutinated forms, ranging from 40% up to 75%. The agglutinated assemblages mainly include trochamminids and tubular forms, whereas *Ammodiscus* sp., *Glomospira* sp., *Dorothia oxycona*, *Dorothia filiformis*, *Gaudryina pyramidata* and *Spiroplectammina* sp. are present in relatively low abundances. Among the calcareous benthic foraminifera, well-preserved aragonitic shells of various species of *Epistomina* are very abundant in some samples. Common calcareous species also include *Lingulogavelinella convexa*, *Berthelina berthelini*, *Epistomina* spp., *Lenticulina* spp., *Gyroidinoides* spp., *Eponides* sp., *Stensioeina* sp., *Gavelinella* sp. and *Colomia*? sp. Less common species are *Pseudosigmoilina* spp., *Quadrimorphina* sp., *Dentalina* sp., *Nodosaria* sp., *Marginulina* sp., *Astacolus* sp., *Tappanina laciniosa*, *Frondicularia* sp., *Psilocitharella* sp., *Saracenaria* sp., *Ceratobulimina* spp., *Pseudopatelinella* sp., *Lagena* sp., *Fissurina* sp. and buliminids. Finally, a strong faunal turnover in the benthic association is observed at the base of the *Marginotruncana schneegansi* Zone (upper Turonian) (Fig. 9), where most of the above-mentioned taxa disappear, agglutinated forms become less abundant, and *Quadrimorphina* sp., *Allomorphina* sp. and other calcareous trochospiral forms dominate the benthic assemblage.

4.5.3. Calcareous nannofossil biostratigraphy

Nannofossil abundance varies throughout this hole, but is generally moderate. Preservation is moderate to good. The samples studied indicate the base of *Zeugrhabdotus biperforatus* at the top of core TDP31/6 and, thus, the upper Turonian subzone UC9b between cores TDP31/1–5 (Fig. 9). The base of *Lithastrinus septenarius* is present in core TDP31/27, which suggests the middle–upper Turonian UC9a between cores TDP31/6–26. The absence of the subzonal datum marker *Lucianorhabdus quadrifidus* from this site means that the base of UC8b cannot be determined. The base of *Eiffellithus eximius* (base of UC8a) is questionable in core TDP31/31, where it has an initial occurrence. It is then absent through the overlying cores TDP31/25–30 and occurs again in core TDP31/24. A taxonomic study is underway to ensure that the distinction between *E. eximius* and the also-recorded *E.* cf. *E. eximius* is reliably made here. The undifferentiated (sub)zones UC6b–7 (lower Turonian) are recognized in cores TDP31/31–62. It is noteworthy that the base of Zone UC7 has not yet been identified in Tanzania due to the apparent absence of *Quadrum gartneri* from the appropriate interval. Finally, the absence of *Helenea chiastia* and *Eprolithus moratus* at the base of the hole indicates the existence of the lowermost Turonian Zone UC6a.

4.5.4. Chemostratigraphy

The $\delta^{13}C_{org}$ values in this site range from −27.1‰ to −20.8‰ (average = −23.2 ± 1.51‰, 1 s.d.). A local minimum observed at the level of the *Whiteinella archaeocretacea–Helvetoglobotruncana helvetica* boundary (106.52 m) (Fig. 9) shows similar features to those seen at TDP Site 30 (Fig. 8) (Section 4.4.4). High-resolution sampling across this zonal boundary allowed detailed characterization of this local minimum, which consists of a 1.7‰ decrease (from ~114 to 104 m) followed by an interval (from ~104 to 95 m), where values fluctuate by ~0.6‰, before recovering to approximately the same values as recorded in the underlying *W. archaeocretacea* Zone (Fig. 9). The $\delta^{13}C_{org}$ profile also exhibits a 5.7‰ decrease from 72.47 to 26.54 m that crosses the *H. helvetica–Marginotruncana schneegansi* boundary (at 34.11 m) followed by a 2.7‰ increase from 26.54 to 5.05 m.

The $\delta^{13}C_{carb}$ profile shows a large range of values from −13.2‰ to 1.1‰ (average = −1.95 ± 2.85‰, 1 s.d.). This high variability is due to the existence of markedly low excursion values in individual samples (Fig. 9) that are inferred to be of diagenetic origin. The lower part of the profile exhibits no clear vertical patterns; however, the upper part shows an ~3‰ negative shift from the upper *Helvetoglobotruncana helvetica* Zone into the *Marginotruncana schneegansi* Zone (Fig. 9). Because the latter trend is similar to that observed in the $\delta^{13}C_{org}$ profile, they may indicate regional to global shifts of carbon among carbon reservoirs. The $\delta^{18}O_{carb}$ values range between −5.4‰ and −2.2‰ (average = −3.68 ± 0.60‰, 1 s.d.). From the bottom of the hole to ~35 m, the $\delta^{18}O_{carb}$ profile remains relatively constant, with few excursions throughout the *Whiteinella archaeocretacea* to middle *H. helvetica* Zones (Fig. 9). No major variations are observed in the $\delta^{18}O_{carb}$ from ~30 m to the top of the hole.

4.6. TDP Site 32

TDP Site 32 was drilled 20 m south of the main road, 4.5 km to the southwest of Lindi (UTM 37L 575115, 8891688) (Fig. 2 of Supplementary material). The main goal was to try to recover intervals younger than the Campanian already been recovered (TDP Site 28, this study; TDP Site 23, Jiménez Berrocoso et al., 2010). The site was chosen by moving downdip from TDP Sites 23 and 28, 2 km and 1 km to the northwest, respectively. The site was drilled to 59 m, with very low recovery from the surface to 17 m, and good recovery from 17 m to the bottom of the hole. Drilling was stopped in sediments assigned to the *Radotruncana calcarata* Zone, when it was apparent that overlap with the other sites had been achieved.

4.6.1. Lithostratigraphy and bulk sediment composition

Lithologies from the surface to 14 m consist of pale yellowish orange, well-lithified, massive grainstones (Fig. 10), which are similar to those recovered in the upper 9.27 m of TDP Site 28 (Figs. 4 and 5a). Core TDP32/6 shows massive, silty claystones, mixed with

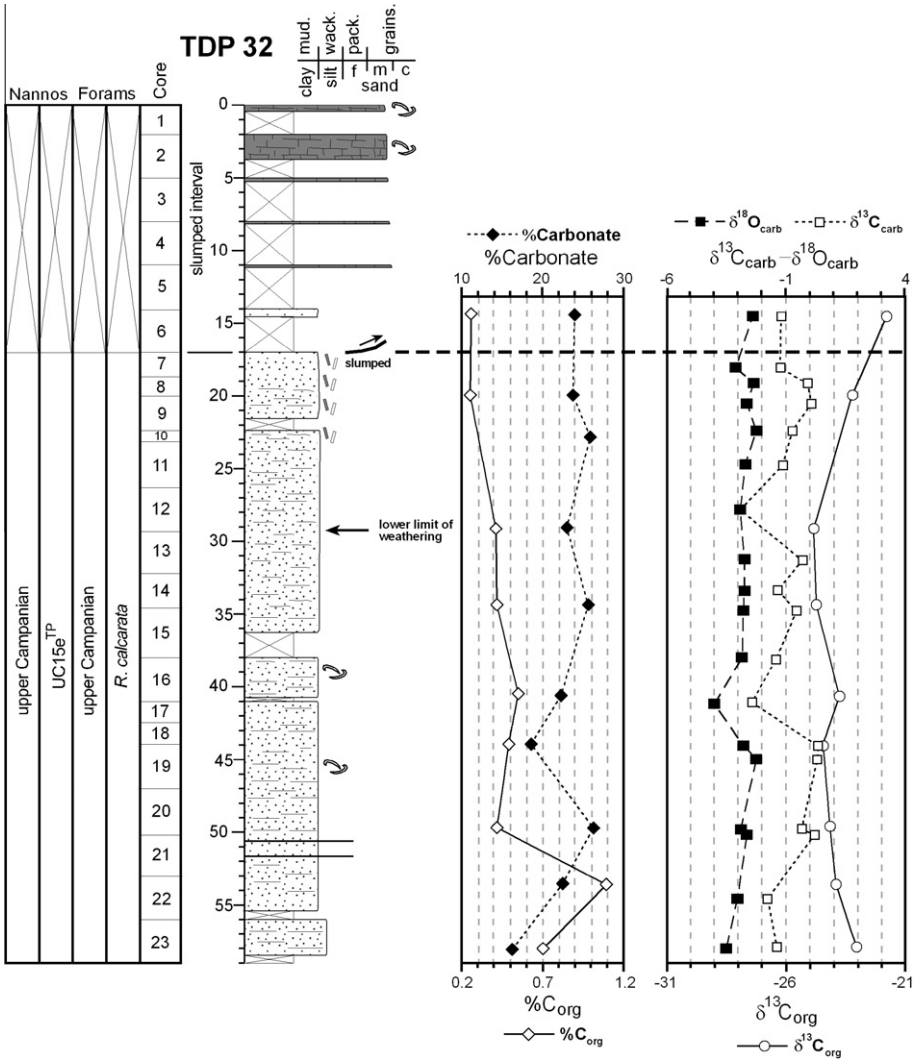

Fig. 10. Integrated lithostratigraphy, planktonic foraminiferal and calcareous nannofossil biostratigraphy, and chemostratigraphy of TDP Site 32. Lower limit of weathering indicated in core 12. Symbols as given in Fig. 2.

drill-mud and fragments of the overlying grainstones, possibly derived from hole caving. Together, this upper section might represent part of a large slump system off the west side of Kitulo Hill (Pearson et al., 2004). All underlying sediments (cores TDP32/7–23) form a monotonous sequence of slightly-laminated, olive gray claystones and greenish gray, silty claystones (Figs. 5c and 10), with sulfate–carbonate vein fractures limited to cores TDP32/7–10. Occasional inoceramid debris is present, but no bioturbation is visible.

The $\%CaCO_3$ in the analyzed bulk sediments from TDP Site 32 ranges from 15.8% to 25.9% (average = 22.48 ± 3.26%, 1 s.d.) and the $\%C_{org}$ from 0.2% to 1.1% (average = 0.49 ± 0.27%, 1 s.d.). In general, the two parameters show an inverse relationship to each other (Fig. 10).

4.6.2. Foraminiferal biostratigraphy

No foraminifera were obtained from the upper six cores of this borehole. Planktonic foraminifera from core TDP32/7 (15.89 m) to the bottom of the hole are abundant and generally show good preservation, with occasional occurrences of glassy shells without infilling. This interval is assigned to the upper Campanian *Radotruncana calcarata* Zone, based on the presence of the nominate taxon (Fig. 10).

Benthic foraminifera are more abundant than planktonic foraminifera in all samples studied from this site, and show a high diversity with a dominance of calcareous over agglutinated forms.

4.6.3. Calcareous nannofossil biostratigraphy

Nannofossil abundance in the samples analyzed from this site varies from low to high, and preservation is moderate to good. The co-occurrence of *Eiffellithus paralellus*, the base of which is the marker for the base of $UC15e^{TP}$, and *E. eximius*, the top of which defines the top of $UC15e^{TP}$, places cores TDP32/7–23 in $UC15e^{TP}$ (Fig. 10). This biozone indicates the upper Campanian, in accordance with the planktonic foraminiferal age.

4.6.4. Chemostratigraphy

A number of similarities can be observed between the isotopic records of the upper part of TDP Site 28 (upper Campanian *Radotruncana calcarata* Zone) (Fig. 4) and those of TDP Site 32, assigned to the same planktonic foraminiferal biozone (Fig. 10). As seen in TDP Site 28, the range of $\delta^{13}C_{org}$ values at TDP Site 32 is from −24.9‰ to −21.9‰ (average = −23.84 ± 0.96‰, 1 s.d.) and there is no systematic trend through the profile. The $\delta^{13}C_{carb}$ values range from −2.9‰ to 0.3‰ (average = −0.92 ± 0.94‰, 1 s.d.) and the vertical profile shows considerable variations, consistent with what is

seen at TDP Site 28. Finally, similar to TDP Site 28 (Fig. 4), the $\delta^{18}O_{carb}$ values in TDP Site 32 range from −4.02‰ to −2.26‰ (average = −2.84 ± 0.43‰, 1 s.d.) and, in general, the vertical profile shows values that are relatively constant (Fig. 10).

4.7. TDP Site 33

TDP Site 33 was drilled 1.8 km west of the main road, 10.3 km to the southwest of Lindi (UTM 37L 568224, 8891149) (Fig. 2 of Supplementary material). The site is 100 m southeast of a surface sample containing the lower Cenomanian foraminiferal marker *Thalmanninella globotruncanoides*. The main goal was to drill the lower Cenomanian and Albian. The site was drilled to 26.20 m, with moderate recovery between the surface and 17.20 m, and low recovery between 17.20 m and the bottom of the hole. Drilling was terminated in a lithified sandstone interval that prevented further penetration.

4.7.1. Lithostratigraphy and bulk sediment composition

The main lithologies from the surface to the bottom of the hole are light olive gray and olive black, massive, clayey siltstones and claystones (Figs. 11 and 12a), with common oxide stains along fractures due to modern weathering. Laminated fabrics are very rare, and no bioclasts are visible. Cores TDP33/4, 12 and 13 present intervals with up to medium-grained, well-lithified sandstones (Fig. 12b–d). Some of the sandstones show mm- to cm-sized, greenish siltstone clasts (Fig. 12b). Core TDP33/11 exhibits a 35-cm-thick, light gray, well-lithified carbonate layer with abundant quartz grains (Fig. 11).

The $\%CaCO_3$ in the analyzed samples from this site varies from 12.0% to 24.2% (average = 19.76 ± 4.31%, 1 s.d.) and the $\%C_{org}$ from 0.2% to 0.6% (average = 0.34 ± 0.13%, 1 s.d.). Neither of them shows apparent trends through the short interval cored (Fig. 11).

4.7.2. Foraminiferal biostratigraphy

Planktonic foraminifera are absent from cores TDP33/1 and 11–13, but present in 2–10, with specimens showing moderate to good preservation and no shell infilling. Cores TDP33/2–10 (3.50–16.41 m) yield a very rare planktonic assemblage assigned to the lower Cenomanian *Thalmanninella globotruncanoides* Zone (Fig. 11), based on the occurrence of the nominate taxon with *T. brotzeni*, *Parathalmanninella appenninica*, *Praeglobotruncana delrioensis*, *Pr. stephani* and *Pr. gibba* and the absence of younger rotaliporids.

4.7.3. Calcareous nannofossil biostratigraphy

The samples analyzed from cores TDP33/11–13 are barren of nannofossils. The remaining interval (cores TDP33/1–10) yields low nannofossil abundance, but preservation is moderate to good. This interval lies within UC3a–b (Fig. 11) (middle–upper Cenomanian), based on the co-occurrence of *Lithraphidites acutus* in the lowermost sample (the base of which marks the base of UC3a) and *Staurolithites gausorhethium* at the top of the interval (the top of which marks the top of UC3b). The marker for the base of UC3b (top of *Gartnerago theta*), is not present in Tanzania, and so these two subzones cannot be differentiated here.

4.7.4. Chemostratigraphy

Only 10 bulk samples from this site were analyzed for stable isotopes. The $\delta^{13}C_{org}$ values range from −23.1‰ to −21.6‰ (average = −22.11 ± 0.34‰, 1 s.d.) and show little variation through the interval studied (Fig. 11). The $\delta^{13}C_{carb}$ values range from −10.9‰ to −1.0‰ (average = −5.17 ± 2.64‰, 1 s.d.) and the $\delta^{18}O_{carb}$ from −5.0‰ to −3.0‰ (average = −3.83 ± 0.53‰, 1 s.d.). Only the lowermost analyzed sample exhibits a very low $\delta^{13}C_{org}$ value (Fig. 11).

4.8. TDP Site 34

TDP Site 34 was drilled 0.4 km west of the main road, 8.7 km to the southwest of Lindi (UTM 37L 569875, 8891254) (Fig. 2 of Supplementary material). The site is 90 m to the east-southeast of a surface sample containing the upper Cenomanian–lower Turonian foraminiferal marker *Whiteinella archaeocretacea*. Goals for this site were to drill the lower Turonian and the Cenomanian–Turonian boundary interval. The site was drilled to 101.11 m, with moderate to poor recovery from the surface to 35 m, and good recovery between 35 m and the bottom of the hole. Drilling was stopped when coring rods ran out at the well-site, without having reached the Cenomanian.

4.8.1. Lithostratigraphy and bulk sediment composition

The main lithologies from 8 m to the bottom of the hole are mm- to cm-thick, interbedded, olive gray, olive black and greenish black, claystones and sandy siltstones (Figs. 7g and 13), in which

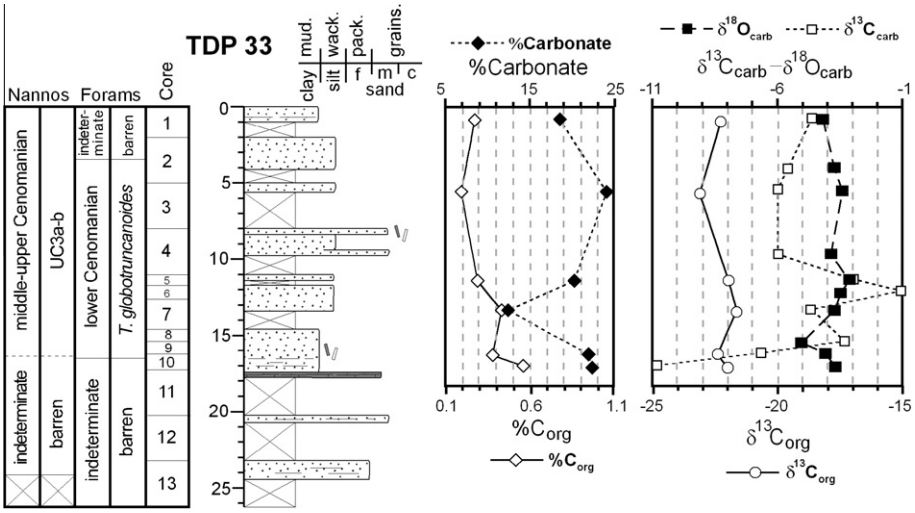

Fig. 11. Integrated lithostratigraphy, planktonic foraminiferal and calcareous nannofossil biostratigraphy, and chemostratigraphy of TDP Site 33. Lower limit of weathering is below core 13. Dashed lines in calcareous nannofossil columns indicate that placement of zonal boundaries is not considered final. Symbols as given in Fig. 2.

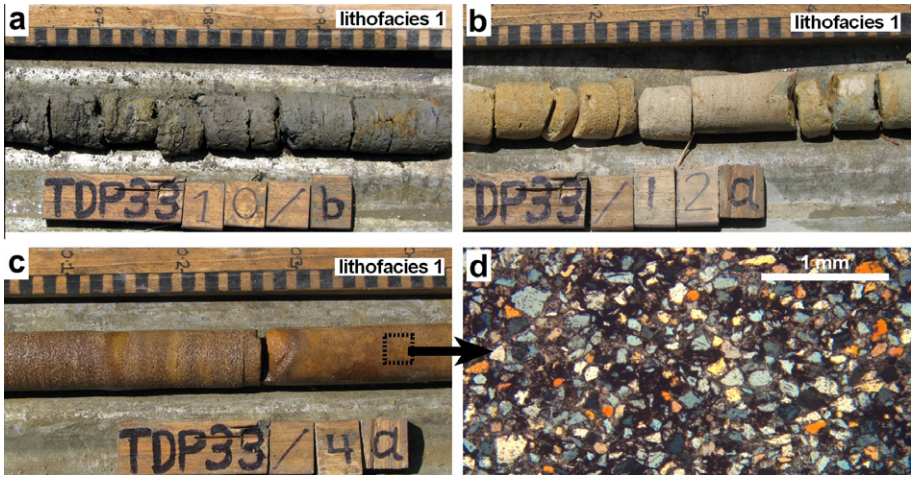

Fig. 12. Photographs of TDP Site 33 (lower Cenomanian). (a) Olive gray, massive claystones with weathering stains along fractures. (b) Fine- to medium-grained sandstones, with greenish siltstone clasts (right-hand side). (c) Reddish brown, fine- to medium-grained sandstones; black, dashed-line rectangle represents position of thin-section in (d). (d) Thin-section view of reddish brown sandstones in (c), in which monocrystalline quartz grains are cemented by calcite and Fe oxides (dark areas between grains). (For interpretation of the references to color in this figure legend, the reader is referred to the web version of this article.)

finely-laminated, possibly organic-rich intervals occur commonly. Cores TDP34/8, 10, 23, 24, 28, 29, 39 and 46 show cm-thick layers of light to medium gray, massive, lithified siltstones (Figs. 7g and 13), with sharp to gradational top and bottom contacts. Light gray, thin sandstone partings are rare in this hole. Yellowish brown, mm- to cm-sized sand nodules and fragments of inoceramid shells are relatively common. Soft-sediment deformation (slightly inclined and convoluted laminations) is observed at intervals from cores TDP34/16–17, 33–38 and 41–44. Lamination is highly disturbed in parts of cores TDP34/36–37 (Figs. 7h and 13).

The $\%CaCO_3$ in this site ranges from 10.2% to 32.3% (average = 18.12 ± 5.35%, 1 s.d.) and, generally, varies inversely with the $\%C_{org}$ (from 0.5% to 1.12%, average = 0.93 ± 0.18%, 1 s.d.) (Fig. 13). An abrupt increase in both $\%CaCO_3$ and $\%C_{org}$ is seen downsection between 11.57 m and 23.07 m. However, there are no apparent stratigraphic intervals in this site that show correlatable $\%CaCO_3$ and $\%C_{org}$ changes with those of TDP Sites 30 and 31 (Figs. 8 and 9), despite all three sites exhibiting similar absolute values and overlapping in time.

4.8.2. Foraminiferal biostratigraphy

Planktonic foraminifera were not recovered from cores TDP34/1–3, and are rare to abundant from core TDP34/4 to the bottom of the hole. All samples studied yield specimens with moderate to excellent preservation and occasional glassy shells. Assemblages from cores TDP34/4–7 are assigned to the lower–middle Turonian *Helvetoglobotruncana helvetica* Zone (Fig. 13), based on the consistent presence of the nominate taxon. The rest of the hole is included in the lower Turonian *Whiteinella archaeocretacea* Zone, due to the absence of *H. helvetica* and Cenomanian rotaliporids, as well as the presence of the nominate taxon alongside evolutionarily advanced forms of *H. praehelvetica*.

Benthic foraminifera from the samples studied in this site average 27% and range from 13% to 53%, relative to planktonic foraminifera. Diversity varies through the section, and the most common taxa include *Lenticulina* spp., *Epistomina* spp., *Lingulogavelinella convexa*, *Gyroidinoides* spp., *Gavelinella* spp., *Berthelina berthelini*, *Stensioeina* sp., *Ammodiscus* sp., *Dorothia oxycona*, *Pseudosigmoilina* sp. and, in some samples, agglutinated trochospiral, planispiral and tubular forms. Less common are *Frondicularia* sp., *Oolina* sp., *Nodosaria* sp., *Dentalina* sp., *Astacolus* sp., *Marginulina* sp., *Saracenaria* sp., *Eponides* sp., *Quadrimorphina* sp., *Tappanina laciniosa*, *Gaudryina* sp., *Spiroplectinata* sp., *Glomospira* sp., *Ramulina* sp., *Colomia*? sp. and buliminids.

4.8.3. Calcareous nannofossil biostratigraphy

The samples studied from this site show very low to moderate nannofossil abundance, with preservation being moderate to good. Only one sample barren of nannofossils was recorded, in core TDP34/8. All these samples fall within the lower Turonian Zone UC6a–b, possibly also UC7 (see comments in Section 4.5.3 about *Quadrum gartneri*), which is in accordance with the planktonic foraminiferal age (Fig. 13).

4.8.4. Chemostratigraphy

The $\delta^{13}C_{org}$ values from this site range from −23.4‰ to −21.0‰ (average = −22.23 ± 0.80‰, 1 s.d.) and show a ~3‰ negative excursion ~23 m below the first appearance of *H. helvetica* (Fig. 13). Negative excursions of 2.5‰ and 1.7‰ were observed in TDP Sites 30 and 31, respectively, but, in these cases, they were bracketing the *Whiteinella archaeocretacea–Helvetoglobotruncana helvetica* boundary (Figs. 8 and 9). The $\delta^{13}C_{carb}$ values in TDP Site 34 range from −10.6‰ to 0.7‰ (average = −1.69 ± 2.72‰,1 s.d.) and, as in TDP Sites 30 and 31, they are relatively consistent through the section except for large, single-point, negative excursions, attributed to diagenetic carbonate. The $\delta^{18}O_{carb}$ values range from −6.2‰ to −3.12‰ (average = −4.02 ± 0.58‰, 1 s.d.) and show negative excursions of up to ~2‰ in the same samples of the large $\delta^{13}C_{carb}$ excursions (Fig. 13), which supports their diagenetic origin. Except for these negative shifts, the $\delta^{18}O_{carb}$ values are relatively constant through the section (similar to those from TDP Sites 30 and 31), suggesting the possibility of preservation of the original isotopic signal.

4.9. TDP Site 35

TDP Site 35 was drilled 50 m east of the main road, 7.5 km to the west of Lindi (UTM 37L 571341, 8893754) (Fig. 2 of Supplementary material). The site is located 77 m to the south-southeast of a surface sample with the foraminiferal marker *Globotruncana ventricosa*. The main goal for this site was to drill through upper Santonian–lower Campanian sediments. The site was drilled to 92 m, with moderate to good recovery from the top to the bottom of the hole. Drilling was stopped on the last day of the 2008 season, with lower Campanian but no Santonian sediments cored.

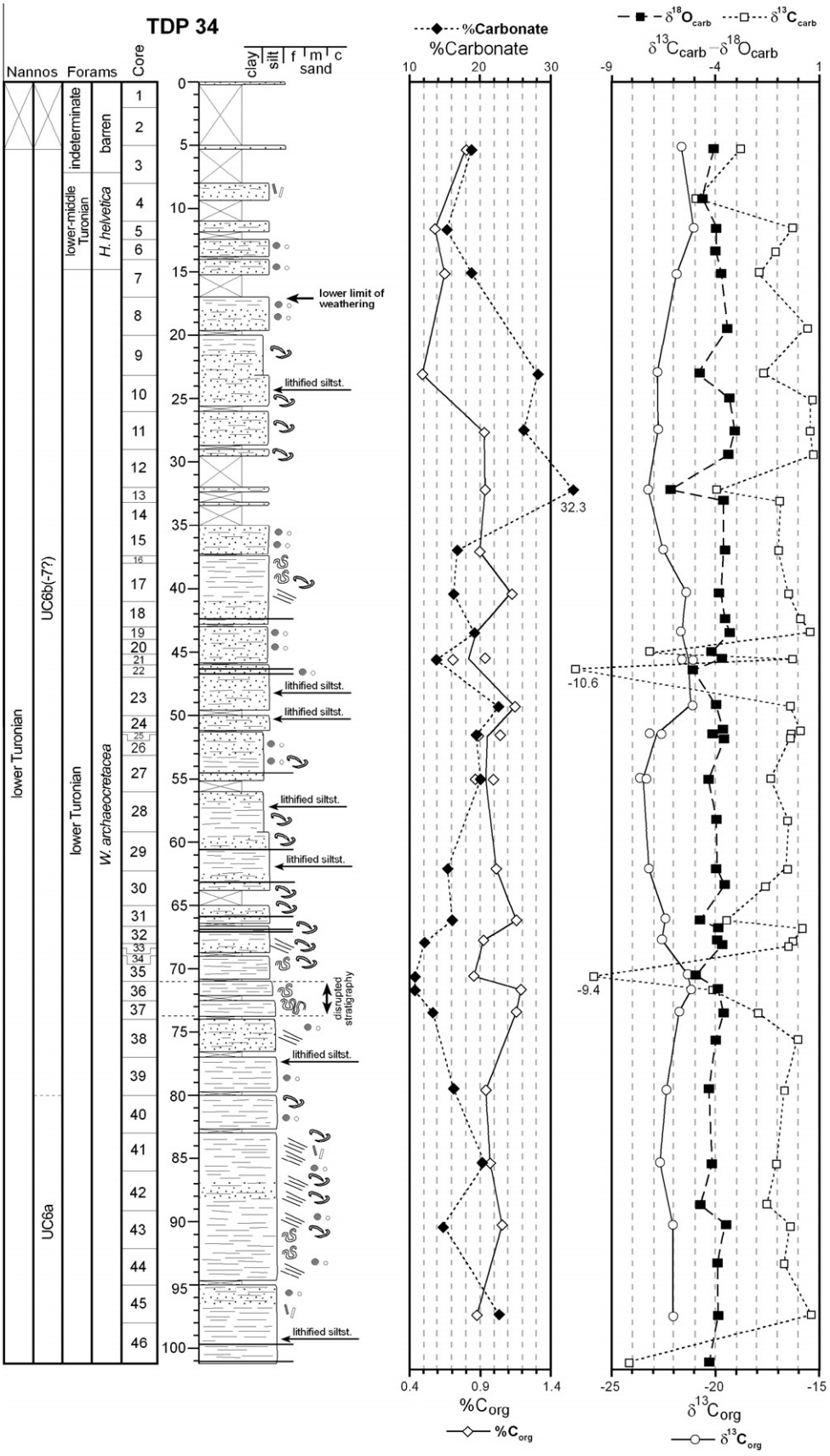

Fig. 13. Integrated lithostratigraphy, planktonic foraminiferal and calcareous nannofossil biostratigraphy, and chemostratigraphy of TDP Site 34. Lower limit of weathering is indicated in core 7. Zone UC6b(-7?) indicates that cores 3–39 possibly covers part of Zone UC7. Dashed lines in calcareous nannofossil columns indicate that placement of zonal boundaries is not considered final. Symbols as given in Fig. 2.

4.9.1. Lithostratigraphy and bulk sediment composition

Underlying a modern soil interval with yellowish orange, semi-lithified sands and claystones (cores TDP35/1), core TDP35/2 to the bottom of the hole show monotonous, greenish gray, occasionally black, massive to slightly-bedded, silty claystones and siltstones (Figs. 5d and 14). Bioturbation is moderate to intense in cores TDP35/8–11 and 16–22, and mainly consists of cm-sized, either oval or elongated burrows, with bedding-subparallel orientation (Fig. 5d). A 14-m-thick interval with abundant bioturbation was also found at the bottom of TDP Site 23 (upper lower Campanian

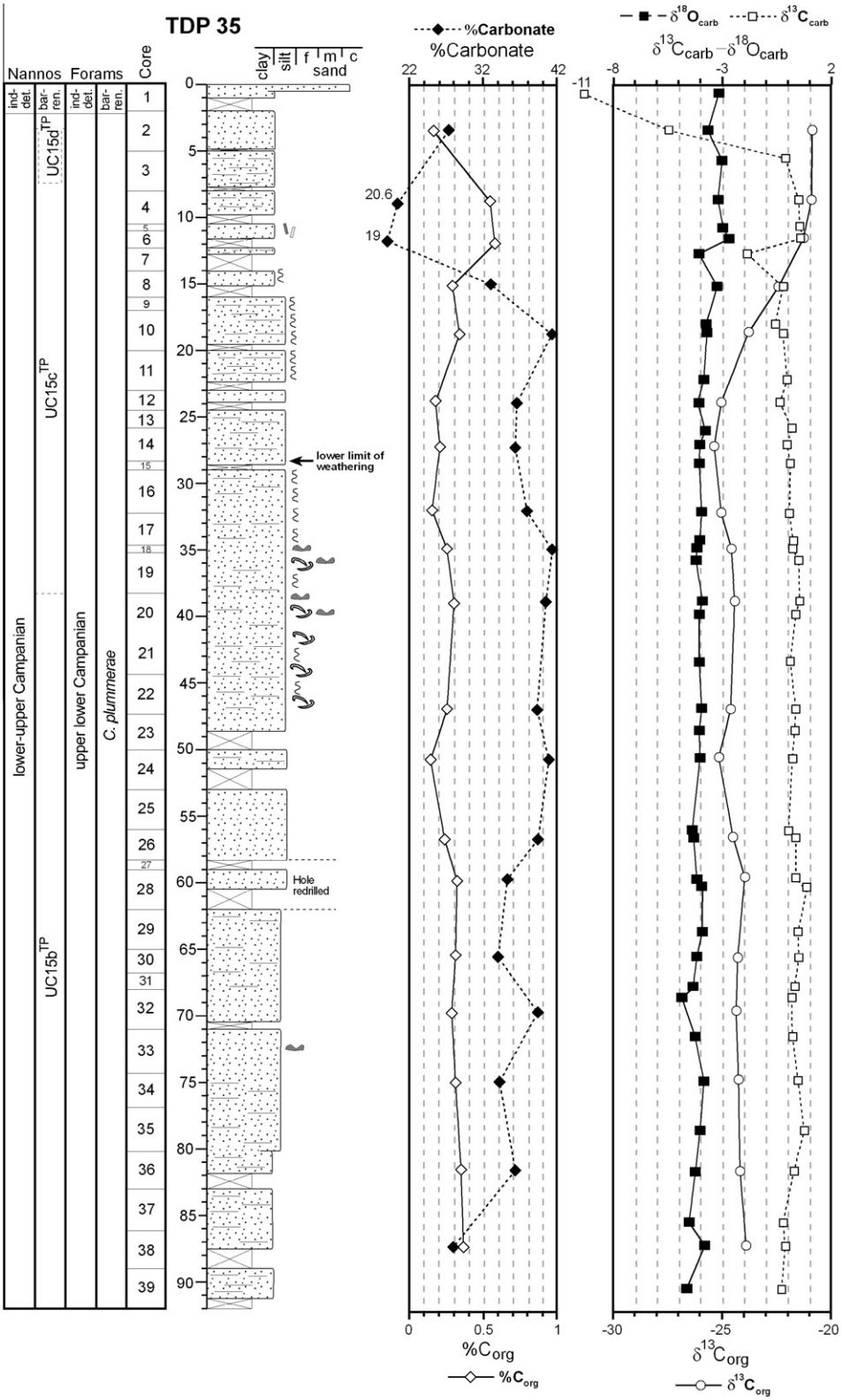

Fig. 14. Integrated lithostratigraphy, planktonic foraminiferal and calcareous nannofossil biostratigraphy, and chemostratigraphy of TDP Site 35. Lower limit of weathering is indicated in core 14. Dashed lines in calcareous nannofossil columns indicate that placement of zonal boundaries is not considered final. Symbols as given in Fig. 2.

Contusotruncana plummerae Zone, according to Petrizzo et al., 2011; previously identified as *Globotruncana ventricosa* Zone in Jiménez Berrocoso et al., 2010), which might represent the lateral equivalent of the bioturbated sediments of TDP Site 35 (Fig. 14). Finally, irregular occurrences of bioclastic debris and disseminated pyrite are visible in cores TDP35/18–22.

The $\%CaCO_3$ in the bulk samples of this site ranges from 19.0% to 41.6% (average = 34.87 ± 6.68%, 1 s.d.) and the $\%C_{org}$ from 0.2% to 0.6% (average = 0.29 ± 0.12%, 1 s.d.). Except for cores TDP35/2–8, which show a strong inverse relationship between $\%CaCO_3$ and $\%C_{org}$ (Fig. 14), these two parameters present relatively constant values through the sections.

4.9.2. Foraminiferal biostratigraphy

Planktonic foraminifera from TDP Site 35 are abundant and very diverse. In general, specimens found show good to moderate preservation, with occasional glassy shells and either pyrite or calcite infilling. Samples from 2.29 m (core TDP35/2) to the bottom of the hole are assigned to the lower part of the *Contusotruncana plummerae* Zone (upper lower Campanian) (Fig. 14), due to both the co-occurrence of the nominate species and the absence of *Radotruncana calcarata*. In addition, specimens of *Globotruncanita elevata* are consistently found in core TDP35/8 to the bottom of the hole, whereas *R. subspinosa* is only observed in cores TDP35/2–7. It is noteworthy that the upper part of the *C. plummerae* Zone (lower upper Campanian) was observed in TDP Site 28 (Fig. 4), where specimens of *G. elevata* were rare but *R. subspinosa* was consistently present.

4.9.3. Calcareous nannofossil biostratigraphy

Apart from a barren sample in core TDP35/1, the rest of the hole contains nannofossils of moderate to high abundance, and generally moderate to good preservation. The lower–upper Campanian is indicated by the presence of *Ceratolithoides aculeus* in the lowermost sample ($UC15b^{TP}$), followed by the bases of *Uniplanarius sissinghii* (marker for the base of $UC15c^{TP}$) and *Uniplanarius trifidus* (marker for the base $UC15d^{TP}$) (Fig. 14).

4.9.4. Chemostratigraphy

The $\delta^{13}C_{org}$ from TDP Site 35 ranges between −25.7‰ and −20.8‰ (average = −23.85 ± 1.41‰, 1 s.d.). This profile shows relatively constant values through the section, except for a broad positive shift in the upper part (cores TDP35/4–12) (Fig. 14). The $\delta^{13}C_{carb}$ values range from −11.0‰ to 0.9‰ (average = −0.16 ± 2.03‰, 1 s.d.). The high standard deviation is due to the existence of two extremely negative values at the top the hole, where a modern soil interval was cored. The $\delta^{18}O_{carb}$ profile ranges from −4.8‰ to −2.7‰ (average = −3.90 ± 0.46‰, 1 s.d.) and shows an overall 1–1.5‰ increase up-section that is consistent with cooling in the Campanian.

4.10. Calcareous dinoflagellates from TDP Sites 29, 30, 31 and 34

Calcareous dinoflagellate cysts have been studied in samples of the Turonian TDP Sites 29–31 and 34. They show a particularly high abundance in the sediments of the lower part of the planktonic foraminiferal *Helvetoglobotruncana helvetica* Zone, with *Pithonella ovalis*, *P. sphaerica* and *Pirumella krasheninnikovii* as the dominant taxa. The assemblage found also contains the rarer pithonelloid *P. atopa*, *P. lamellata*, *P. discoidea*, *P. perlonga*, *P. microgranula* and *Normandia circumperforata*, as well as forms of *Carinellum* sp., *Pi loeblichi*, *Pi. pachystrata*, *Pi. porata*, *Pi. spinosa*, *Orthopithonella* cf. *O. gustafsoni* and two previously unknown species. Assemblages dominated by *P. ovalis* and *P. sphaerica* have been frequently observed in low-latitude (Dias-Brito, 2000) to northern mid-latitude locations (Wendler et al., 2002). A similar pattern found here indicates the Turonian TDP sediments represent a new southern mid-latitude occurrence of the *Pithonella*-dominated calcareous dinoflagellate zone of Dias-Brito (2000). Further, the predominance of *P. ovalis* over *P. sphaerica* in the samples studied suggests an outer shelf-upper slope setting (Wendler et al., 2002), which agrees well with the inferences from sedimentology (Section 5.1) and benthic foraminifera (Section 5.4).

The majority of the specimens observed are exceptionally well-preserved and morphological characteristics can be studied in unprecedented detail. Lath-shaped, ~0.1-μm-sized crystals form the basic building units of the walls of *Pithonella*. These structures have previously been observed only rarely and led to the description of new species (Keupp, 1990). The Tanzanian material studied shows that all pithonelloid species consist of such sub-μm-sized crystals; thus, it questions the distinction of species based on this crystallographic feature. For example, *P. sphaerica* is represented by a wide size-range in the Turonian TDP sites, with maximum and minimum diameters of ~180 μm and ~25 μm, respectively.

5. Discussion

5.1. Lithofacies and sedimentary conditions

The lithologies of the Cretaceous sites drilled in 2007 were grouped into lithofacies 1–5 (Jiménez Berrocoso et al., 2010), according to variations in texture, grain size, color and sedimentary structures. Similarly, the lithostratigraphy of the Cretaceous sites presented in this work reveals vertical successions of varying lithologies that can be grouped into lithofacies 1, 2 and 5.

Lithofacies 1 represents the entire section of TDP Site 33 (Fig. 11) and consists of massive, clayey siltstones and claystones, with cm- to dm-thick intervals of up to medium-grained, massive, well-lithified sandstones, containing occasional mm- to cm-sized, greenish, soft siltstone clasts (Fig. 12a–c). A thin-section from a sandstone layer in core TDP33/4 (Fig. 12c and d) reveals a grain-supported microfabric cemented by calcite, with up to >90%, angular to sub-angular, monocrystalline, fine- to medium-grained quartz. Feldspars and clay minerals form <10% of this microfabric.

Lithofacies 1 was interpreted as evidence of high-energy events that could have originated from turbulent flows (Jiménez Berrocoso et al., 2010). In TDP Site 33, the existence of intervals with up to medium-grained sandstones with soft clasts (Fig. 12b and c) supports this interpretation and suggests flows that possibly transported sand from shallower areas and ripped up clasts from a semi-lithified seafloor. Surface observations in the area of TDP Site 33 reveal the existence of discontinuous layers of cross-laminated, fine- to medium-grained sandstones with flute marks at the base that might represent small channelized bodies (~5–10 m across) equivalent to the medium-grained sandstones cored in this site. Also, the existence of >90% quartz grains in a thin-section of a sandstone from TDP Site 33 (Fig. 12c and d) suggests that transport of sediments occurred across a sufficient distance for removal of a large proportion of less resistant minerals (e.g., feldspars and clays).

Lithofacies 2 occurs in the entire sections of TDP Sites 29–31 and 34 (Figs. 6, 8, 9 and 13). The dominant lithologies are mm- to cm-thick interbeddings of mostly dark gray claystones and sandy siltstones (Fig. 7c–e and g), with no bioturbation, but with sporadic to common ammonite, inoceramid and gastropod remains. Finely-laminated, possibly organic-rich intervals are common (Fig. 7e). Light gray, cm-thick, well-lithified siltstone layers, with sharp to gradational top and bottom contacts, are a minor lithology (Fig. 7a). A thin-section from one of these layers in TDP Site 29 shows a grain-supported microfabric cemented by calcite, with >90% monocrystalline, angular to sub-angular quartz grains and <10% feldspars and clay minerals (Fig. 7a and b). Also, a few beds

of olive black, cm-thick, well-lithified siltstones with horizontal lamination are visible (Fig. 7d). A thin-section from one of the latter beds in TDP Site 30 presents a quartz-cemented, grain-supported microfabric, with >80% monocrystalline, angular to sub-angular quartz grains and <20% clay minerals and feldspars (Fig. 7f). Finally, soft sediment deformation is absent from TDP Site 29, but it is expressed in parts of TDP Sites 30, 31 and 34 as inclined and convoluted lamination (Fig. 7h) or as highly-disturbed lamination (Figs. 8, 9 and 13).

The predominance of clay- and fine sand-sized grains in lithofacies 2 of TDP Sites 22, 24, 24B and 26, along with the occurrence of common calcareous planktonic microfossils and sporadic ammonite and inoceramid remains, was interpreted as evidence of fully-open marine conditions (Jiménez Berrocoso et al., 2010). The abundance of clay- and silt-sized grains and the presence of similar micro- and macrofossils, in lithofacies 2 of TDP Sites 29–31 and 34 support this interpretation. Also, the absence of sedimentary structures suggests sedimentation below the storm-wave base in an outer-shelf setting, in which the main depositional mechanism was probably surface- to mid-water flows that held fine particles in suspension until dilution of the flow allowed the sediment to settle. Some of the washed residues from these sites, however, show abundant angular, silt-sized quartz and heavy minerals (e.g., TDP Site 30) that suggest bottom currents brought sediments offshore from shallower areas. The abundance of detrital angular quartz is higher in the washed residues of TDP Site 34, which might indicate closer proximity to the sediment sources. Further, the presence of well-lithified (carbonate- and quartz-cemented) siltstone layers (80–90% quartz grains) in lithofacies 2 (Fig. 7a, d, and g) is consistent with the existence of bottom currents that transported sediments to the depositional area of this lithofacies.

On the other hand, soft-sediment deformation was observed in lithofacies 2 of TDP Site 22 (lower–middle Turonian) (Jiménez Berrocoso et al., 2010) and it is now confirmed in lithofacies 2 of TDP Sites 30, 31 and 34 (Figs. 7h, 8, 9, and 13). That is, the soft deformation is most common in parts of the lower–middle Turonian (*Whiteinella archaeocretacea* to middle part of *Helvetoglobotruncana helvetica* Zones) at least near Lindi. Lateral correlation of the intervals with soft deformation is difficult to demonstrate, due to the lack of marker beds; however, because this deformation occurs in the majority of the sites of this age, its cause could be a significant feature that intermittently affected at least part of this basin during this time interval. The reasons for relatively common deformation in this interval will be subjected to further study, but might include high sedimentation rates leading to slump-prone deposits perhaps remobilized by earthquakes and/or bottom-current action before compaction took place. Regardless of the main reason, the stratigraphy of the sediments cored is only disrupted within the intervals with intense deformation (Fig. 7h) of TDP Sites 30 and 34 (Figs. 8 and 13). Thus, the vast majority of the cored sediments from the Turonian sites should yield reliable paleoceanographic and paleoclimatic information.

Lithofacies 5 is assigned to the Campanian interval drilled in TDP Sites 28, 32 and 35 (Figs. 4, 10 and 14) and consists of olive gray to olive black and greenish gray, monotonous, silty claystones and siltstones (Fig. 5b–d). These sediments mainly have a massive texture, although slightly laminated intervals are also observed. Light gray, sandy partings are relatively common. Bioclastic debris (e.g., inoceramids) and bioturbation in this lithofacies are generally rare. Only limited intervals of TDP Site 35 show frequent, cm-sized, bedding-subparallel burrows (Figs. 7d and 14).

Lithofacies 5 of TDP Site 23 was interpreted as evidence of deposition on an outer-shelf setting below the storm-wave base, due to the dominance of clay-sized grains, the existence of calcareous planktonic microfossils, ammonite and inoceramid remains, and the absence of sedimentary structures (Jiménez Berrocoso et al., 2010). The abundance of clay- and silt-sized grains in lithofacies 5 of TDP Sites 28, 32 and 35, and the presence of planktonic and inoceramid debris support this interpretation. The main depositional mechanism was probably fine-particle settling, with only some bottom-current pulses introducing fine sand offshore. Finally, frequent bioturbation burrows in intervals of TDP Site 35 (upper lower Campanian of the *Contusotruncana plummerae* Zone) suggest periods of favorable nutrients and/or oxygen levels for burrowing activity. Abundant bioturbation in an interval of similar age in TDP Site 23 (Jiménez Berrocoso et al., 2010) may suggest these intervals represent lateral equivalents and a time of favorable conditions for benthic activity, at least, in part of this basin near Lindi.

5.2. Planktonic foraminiferal biostratigraphy

Planktonic foraminiferal marker species are present in most of the samples studied and indicate our sediments span part of the lower Cenomanian through upper Campanian, in addition to a thin interval of the middle Paleocene.

Turonian planktonic foraminifera are of particular interest to our work because they indicate that TDP Site 31 is the most biostratigraphically complete Turonian sequence found during TDP drilling. This site ranges from the lower Turonian *Whiteinella archaeocretacea* Zone through the upper Turonian–Coniacian *Dicarinella concavata* Zone (Fig. 9) and overlaps with TDP Sites 29, 30, 34 (this work) (Figs. 6, 8 and 13), and 22 (Jiménez Berrocoso et al., 2010), which cover the *W. archaeocretacea* to *Helvetoglobotruncana helvetica* Zones. Calculations based on planktonic foraminiferal data suggest a sedimentation rate of 37.4 m/Myr for TDP Site 31. Also, shell preservation in this site is good to excellent through the interval from the *W. archaeocretacea* to *H. helvetica* Zones and moderate through the *Marginotruncana schneegansi* to *D. concavata* Zones. Further, foraminiferal preservation is often good to excellent in the other Turonian sites. Together, these sites provide an unprecedented opportunity to study biostratigraphy and temperature records from a southern subtropical location.

Another striking feature of our Turonian sites is the existence of a comparatively thick *Whiteinella archaeocretacea* Zone. A relatively short duration of ~0.6 Myr is generally assigned to the time of deposition of this biozone (Gradstein et al., 2004), which is difficult to reconcile with the large thickness of 75.15 and 85.63 m attributed to this biozone in TDP Sites 30 and 34, respectively (Figs. 8 and 13). Either a delayed first appearance of *Helvetoglobotruncana helvetica* or an unusually high sedimentation rate must be invoked to explain this expanded *W. archaeocretacea* Zone.

Finally, Santonian to upper Campanian planktonic foraminifera, ranging from the *Dicarinella asymetrica* to *Radotruncana calcarata* Zones, have been recovered from TDP Site 28 (Fig. 4). These specimens show moderate to good preservation and indicate the existence of a ~6 Myr unconformity that separates the upper part of the *Contusotruncana plummerae* Zone (lower upper Campanian) from the underlying *D. asymetrica* Zone (Santonian) (Fig. 4). Interestingly, TDP Sites 35 (this study) and 23 (Jiménez Berrocoso et al., 2010), which were drilled ~3–1 km away from TDP Site 28, show planktonic foraminifera with moderate to good preservation assigned to the lower part of the *C. plummerae* Zone (upper lower Campanian) (Jiménez Berrocoso et al., 2010; Petrizzo et al., 2011; this study). That is, the sequence missing in TDP Site 28 was at least partly recovered in the nearby TDP Sites 35 and 23, and suggests significant sedimentation rate changes or structural complications affecting the Santonian–Campanian near Lindi.

5.3. Calcareous nannofossil biostratigraphy

Apart from problems associated with recognizing the base of UC7 (base *Quadrum gartneri*) in the lower Turonian, all expected

markers are present. The *Q. gartneri* 'problem' is under investigation as part of a wider Cenomanian–Turonian boundary study. Nannofossil biostratigraphy indicates that the 2008 season drilled sediments spanning the middle–upper Cenomanian (Site 33), lowermost (Sites 29, 31, 34) and lower–upper Turonian (Sites 30, 31, 34), middle–upper Santonian (Site 28), lower (Site 35) and upper Campanian (Sites 28, 32, 35) and Selandian (middle Paleocene) (Site 27). Generally, the nannofossil biostratigraphy accords with the planktonic foraminiferal biostratigraphy, although some of the substage assignments do not show good agreement (e.g., Sites 31, 33, 35). In the Campanian, the nannofossils are poorly calibrated with the substages at low latitudes, as are the foraminifera. Our ongoing work involves better calibrating the nannofossil and foraminifera datum with each other, and with independent stratigraphies, so as to overcome these apparent discrepancies.

Preservation at most of the 2008 sites is moderate to good, and a number of new species will be described elsewhere. Data on the biodiversity through the Upper Cretaceous, and results of a study on the environmental shifts indicated by changes in nannofossil abundances, particularly in the Cenomanian and lower Turonian, based on both light microscope and scanning electron microscope observations, will also be published elsewhere.

5.4. Benthic foraminifera and paleo-water depth

Benthic foraminiferal assemblages from our Turonian sites are very similar and indicate an outer shelf-upper slope setting, at a few hundred meters of water depth. Washed residues from the lowermost cores of TDP Site 30 (*Whiteinella archaeocretacea* Zone) (Fig. 8) contain middle-outer shelf assemblages that, together with abundant gastropods and echinoid fragments, suggest a slightly shallower setting during the early Turonian at this location.

A benthic foraminiferal turnover has been observed between cores 19 and 18 of TDP Site 31 (Fig. 9) that indicates shallowing in the late Turonian *Marginotruncana schneegansi* Zone. This turnover is associated with a strong increase in the abundance of biserial planktonic foraminifera and with an increase in the sediment grain size.

The Campanian TDP Sites 28, 32 and 35 (Figs. 10 and 14) show a high diversity of benthic foraminifera, with mostly calcareous species, and a dominance of benthic versus planktonic species. Low abundance of agglutinated forms and lower relative abundance of planktonic foraminifera in the Campanian sites may suggest slightly shallower water depths than for the Turonian sites.

5.5. Chemostratigraphic trends

Several bulk isotopic trends are apparent in the Cretaceous TDP sites. The $\delta^{13}C_{org}$ seems to show a consistent shift at similar stratigraphic intervals in different sites, most notably the broad negative excursion present at, or just below, the *Whiteinella archaeocretacea–Helvetoglobotruncana helvetica* boundary in TDP Sites 30, 31 and 34 (Figs. 8, 9 and 13). Yet, the lack of obvious parallels to the expected global patterns (e.g., Jarvis et al., 2006) makes any interpretation difficult. That is, local processes in this region could have had a greater impact on the bulk isotopic record than global trends. Possibilities of local processes include variations in primary production rates or shifting contributions of terrestrial and marine organic matter. The $\delta^{13}C_{carb}$ values are consistent with this interpretation and generally show lower values than expected for an open-ocean setting. The $\delta^{18}O_{carb}$ values, on the other hand, are consistently between −4‰ and −4.5‰ through the Turonian TDP Sites 29–31 and 34 (Figs. 6, 8, 9 and 13) and increase gradually to values of about −3‰ in the Campanian TDP Sites 28, 32 and 35 (Figs. 4, 10 and 14). These $\delta^{18}O_{carb}$ trends parallel expected shifts based on Late Cretaceous global temperature trends and would yield temperatures of ~26–32 °C using standard assumptions for Late Cretaceous temperature estimates.

Many individual $\delta^{13}C_{carb}$ and $\delta^{18}O_{carb}$ values are notably low suggesting a diagenetic overprint. This overprint is due to recrystallization in the presence of meteoric waters in the upper portions of the sections and to local incorporation of remineralized organic carbon during burial diagenesis in deeper parts of the cores. In these sections, the $\delta^{13}C_{carb}$ values seem to be more often and more extremely offset than the $\delta^{18}O_{carb}$ values. Such a pattern is opposite to that seen in deep-sea carbonates, but is consistent with the relatively low carbonate content of many of our samples (that is, the measured $\delta^{13}C_{carb}$ values are not buffered by a high biogenic carbonate content). Further, the shallow burial proposed for the sediments in this region (e.g., Pearson et al., 2004, 2006) would mean diagenetic carbonate was likely formed at temperatures not too different from those at the sea floor minimizing the offset in $\delta^{18}O_{carb}$ values. Diagenetic alteration was apparently quite localized, and altered samples are most common and dramatically offset in the Turonian sediments, where veins of diagenetic sulfate–carbonate are also relatively common.

6. Concluding remarks

The 2008 TDP drilling season provided eight new Upper Cretaceous sites (along with a thin Paleocene section) that confirm the existence of a much more expanded and complete Upper Cretaceous sequence than previously documented in southeastern coastal Tanzania.

Lithologies from the new sites consist of thick claystone and siltstone intervals, with locally abundant finely-laminated fabrics, sporadic cm- to mm-thick fine sandstone layers, and irregular occurrences of inoceramids, ammonites and gastropods, but common planktonic and benthic microfossils (foraminifera, calcareous nannofossils and dinoflagellates). These intervals present a high range of $CaCO_3$ (~5–40%) and C_{org} content (~0.1–2%), the latter showing higher values in the Turonian, which may be of interest for petroleum exploration. Minor lithologies include much thinner intervals of up to medium-grained, massive sandstones with rare, soft clasts. All these lithologies have been grouped into different lithofacies that indicate deposition of the sediments varied between outer shelf and upper slope settings in a subtropical, continental margin. The main depositional mechanism was fine-particle (clay- and silt-sized) settling, with minor occurrences of bottom currents (e.g., turbulent flows) transporting coarser sediments. Outer shelf-upper slope settings, in a few hundred meters of water depth, are supported by the benthic foraminiferal assemblages observed. According to these assemblages, a slightly shallower setting could have existed in the Campanian, compared to the Turonian.

Planktonic foraminifera from the new TDP sites exhibit excellent preservation in the majority of the samples from the Turonian and, less frequently in some intervals of the Cenomanian and Campanian. TDP Site 31 is the most biostratigraphically complete Turonian section found during TDP drilling. This site spans the lower Turonian–Coniacian (*Whiteinella archaeocretacea–Dicarinella concavata* Zones) and overlaps with the lower–middle Turonian cored in TDP Sites 29, 30 and 34 (*W. archaeocretacea–Helvetoglobotruncana helvetica* Zones). Discontinuous sections of the Santonian–upper Campanian (*D. asymetrica–Radotruncana calcarata* Zones) were collectively recovered from TDP Sites 28, 32 and 35. In addition, thin sequences of the lower Cenomanian (*Thalmanninella globotruncanoides* Zone) and middle Paleocene (P3a Zone) were cored in TDP Sites 33 and 27, respectively.

The nannofloras generally show good preservation and high species richnesses, with small, delicate heterococcoliths and

holococcoliths being common components of the assemblages. The nannofossil biostratigraphy is in general agreement with that derived from the planktonic foraminifera. Several studies are in progress that will be published elsewhere.

The bulk sediment isotopic records of the new TDP sites show largely stable vertical profiles. Only some of the $\delta^{13}C_{org}$ shifts seem to occur at similar intervals in different Turonian sites and the lack of shifts paralleling global patterns published elsewhere, though, suggests that local processes could be more influential than global trends in our bulk organic carbon isotopic ratios. The $\delta^{13}C_{carb}$ records are consistent with this interpretation, and they show lower values than expected for an outer-shelf setting. The $\delta^{18}O_{carb}$ records show a shift from $\sim -4‰$ in the Turonian to $\sim -3‰$ in the Campanian and suggest preservation of global patterns reflecting Late Cretaceous cooling from the Turonian into the Campanian. Superimposed on these trends, the $\delta^{13}C_{carb}$ and $\delta^{18}O_{carb}$ profiles exhibit sharp negative excursions which suggest localized diagenetic alteration due to weathering in the presence of meteoric waters and/or local incorporation of remineralized organic carbon during burial diagenesis.

Acknowledgments

The Tanzania Petroleum Development Corporation and the Tanzania Commission for Science and Technology are acknowledged for logistical support and permission to carry out this research in the field. We appreciate the generous hospitality and valuable technical assistance of Ephrem Mchana, the late Michael Mkereme, and Elvis Mgaya (Mr. K). Field work and drilling were funded by a USA National Science Foundation grant to KGM and BTH (EAR 0642993) and a Smithsonian Walcott Fund grant to BTH. JAL was funded by the NERC (Grant NE/G004986/1). Financial support to MRP was provided by MIUR-Prin 2007-2007W9B2WE 001. The PhD program of the Università degli Studi di Milano is acknowledged for funding FF. All authors participated in the 2008 drilling season. AJB did the sedimentological and facies analysis. BTH, MRP, HC, FF, HB and LC did the planktonic foraminiferal biostratigraphy. JAL and PRB did the calcareous nannofossil biostratigraphy. IW and JW did the benthic foraminiferal and dinoflagellates analyses, respectively. KGM and SH carried out the chemostratigraphic measurements. AJB, BTH, KGM, MRP, JAL, HC, HB, IW, JW, PRB and SH collaborated on writing the manuscript.

Appendix A. Supplementary material

Supplementary data associated with this article can be found, in the online version, at http://dx.doi.org/10.1016/j.jafrearsci.2012.05.006.

References

Bernaola, G., Martin-Rubio, M., Baceta, J.I., 2009. New high resolution calcareous nannofossil analysis across the Danian/Selandian transition at the Zumaia section: comparison with South Tethys and Danish sections. Geologica Acta 7 (1–2), 79–92.

Bown, P.R., 2005. Palaeogene calcareous nannofossils from the Kilwa and Lindi areas of coastal Tanzania (Tanzania Drilling Project 2003–2004). Journal of Nannoplankton Research 27, 21–95.

Bown, P.R., Dunkley Jones, T., 2006. New Palaeogene calcareous nannofossil taxa from coastal Tanzania: Tanzania Drilling Project Sites 11 to 14. Journal of Nannoplankton Research 28, 17–34.

Bown, P.R., Lees, J.A., Young, J.R., 2004. Calcareous nannofossil evolution and diversity through time. In: Thierstein, H.R., Young, J.R. (Eds.), Coccolithophores: From Molecular Process to Global Impact. Springer-Verlag, pp. 481–508.

Bown, P.R., Dunkley Jones, T., Lees, J.A., Pearson, P.N., Randell, R., Coxall, H.K., Mizzi, J., Nicholas, C., Karega, A., Singano, J., Wade, B.S., 2008. A calcareous microfossil Konservat-Lagerstätte from the Paleogene Kilwa Group of coastal Tanzania. GSA Bulletin 120, 3–12.

Burnett, J.A., with contributions from Gallagher, L.T. and Hampton, M.J., 1998. Upper Cretaceous. In: Bown, P.R. (Ed.), Calcareous Nannofossil Biostratigraphy. British Micropalaeontological Society Series. Chapman & Hall/Kluwer Academic Press, pp. 132–199.

Bybell, L.M., Self-Trail, J.M., 1995. Evolutionary, Biostratigraphic, and Taxonomic Study of Calcareous Nannofossils from the Continuous Paleocene–Eocene Boundary Section in New Jersey. US Geological Survey Professional Paper 1554, pp. 36.

Dias-Brito, D., 2000. Global stratigraphy, palaeobiogeography and palaeoecology of Albian–Maastrichtian pithonellid calcispheres: impact on Tethys configuration. Cretaceous Research 21, 315–349.

Ernst, G., Schlüter, T., 1989. The Upper Cretaceous of the Kilwa Region, Coastal Tanzania. Workshop Geol. Tanzania Rev. Res. Progr. University of Köln, Abstr., Cologne, pp. 1–3.

Ernst, G., Zander, J., 1993. Stratigraphy, facies development, and trace fossils of the Upper Cretaceous of southern Tanzania (Kilwa District). In: Geology and Mineral Resources of Somalia and Surrounding Areas, Inst. Agron. Oltremare Firenze, Relaz. E Monogr. 113, Firenze, pp. 259–278.

Falzoni, F., Petrizzo, M.R., 2011. Taxonomic overview and evolutionary history of *Globotruncanita insignis* (Gandolfi, 1955). Journal of Foraminiferal Research 41, 371–383.

Gierlowski-Kordesch, E., Ernst, G., 1987. A flysch trace assemblage from the Upper Cretaceous shelf of Tanzania. In: Matheis, G., Schandelmeier, H. (Eds.), Current Research in African Earth Sciences, pp. 217–222.

Gradstein, F.M., Ogg, J.G., Smith, A.G. (Eds.), 2004. A Geologic Time Scale 2004. Cambridge Univ. Press, New York, 589 pp.

Handley, L., Pearson, P.N., McMillan, I.K., Pancost, R.D., 2008. Large terrestrial and marine carbon and hydrogen isotope excursion in a new Paleocene/Eocene boundary section from Tanzania. Earth and Planetary Science Letters 275, 17–25.

Huber, B.T., MacLeod, K.G., Tur, N.A., 2008. Chronostratigraphic framework for Upper Campanian–Maastrichtian sediments on the Blake Nose (subtropical North Atlantic). Journal of Foraminiferal Research 38, 162–182.

Jarvis, I., Gale, A.S., Jenkyns, H.C., Pearce, M.A., 2006. Secular variation in Late Cretaceous carbon isotopes: a new $\delta^{13}C$ carbonate reference curve for the Cenomanian–Campanian (99.6–70.6 Ma). Geological Magazine 143, 561–608.

Jiménez Berrocoso, Á., MacLeod, K.G., Huber, B.T., Lees, J.A., Wendler, I., Bown, P.R., Mweneinda, A.K., Isaza Londoño, C., Singano, J., 2010. Lithostratigraphy, biostratigraphy and chemostratigraphy of Upper Cretaceous sediments from southern Tanzania: Tanzania drilling project sites 21–26. Journal of African Earth Sciences 57, 47–69.

Kent, P.E., Hunt, J.A., Johnstone, D.W., 1971. The Geology and Geophysics of Coastal Tanzania. Institute of Geological Sciences Geophysical Paper No. 6, i–vi, 1–101. HMSO, London.

Keupp, H., 1990. A new pithonelloid calcareous dinoflagellate cyst from the upper Cretaceous of South Dakota/USA. Facies 22, 47–58.

Key, R.M., Smith, R.A., Smelor, M., Sæther, O.M., Thorsnes, T., Powell, J.H., Njange, F., Zandamela, E.B., 2008. Revised lithostratigraphy of the Mesozoic–Cenozoic succession of the onshore Rovuma Basin, northern coastal Mozambique. South African Journal of Geology 111, 89–108.

Lees, J.A., 2007. New and rarely reported calcareous nannofossils from the Late Cretaceous of coastal Tanzania: outcrop samples and Tanzania Drilling Project Sites 5, 9 and 15. Journal of Nannoplankton Research 29, 39–65.

Martini, E., 1971. Standard Tertiary and Quaternary calcareous nannoplankton zonation. In: Farinacci, A. (Ed.), Proceedings of the Second Planktonic Conference Roma 1970, vol. 2, Edizioni Tecnoscienza, Rome, pp. 739–785.

Moore, W.R., McBeath, D.M., Linton, R.E., Terris, A.P., Stoneley, R., 1963. Geological Survey of Tanganyika Quarter Degree Sheet 256 & 256E. 1:125 000 Kilwa. first ed. Geological Survey Division, Dodoma.

Nicholas, C.J., Pearson, P.N., Bown, P.R., Dunkley Jones, T., Huber, B.T., Karega, A., Lees, J.A., McMillan, I.K., O'Halloran, A., Singano, J., Wade, B.S., 2006. Stratigraphy and sedimentology of the Upper Cretaceous to Paleogene Kilwa Group, southern coastal Tanzania. Journal of African Earth Sciences 45, 431–466.

Nicholas, C.J., Pearson, P.N., McMillan, I.K., Ditchfield, P.W., Singano, J.S., 2007. Structural evolution of coastal Tanzania since the Jurassic. Journal of African Earth Sciences 48, 273–297.

Pearson, P.N., Ditchfield, P.W., Singano, J., Harcourt-Brown, K.G., Nicholas, C.J., Olsson, R.K., Shackleton, N.J., Hall, M.A., 2001. Warm tropical sea surface temperatures in the Late Cretaceous and Eocene epochs. Nature 413, 481–487.

Pearson, P.N., Nicholas, C.J., Singano, J.M., Bown, P.R., Coxall, H.K., van Dongen, B.E., Huber, B.T., Karega, A., Lees, J.A., Msaky, E., Pancost, R.D., Pearson, M., Roberts, A.P., 2004. Paleogene and Cretaceous sediment cores from the Kilwa and Lindi areas of coastal Tanzania: Tanzania Drilling Project Sites 1–5. Journal of African Earth Sciences 39, 25–62.

Pearson, P.N., Nicholas, C.J., Singano, J.M., Bown, P.R., Coxall, H.K., van Dongen, B.E., Huber, B.T., Karega, A., Lees, J.A., MacLeod, K., McMillan, I.K., Pancost, R.D., Pearson, M., Msaky, E., 2006. Further Paleogene and Cretaceous sediment cores from the Kilwa area of coastal Tanzania: Tanzania Drilling Project Sites 6–10. Journal of African Earth Sciences 45, 279–317.

Pearson, P.N., van Dongen, B.E., Nicholas, C.J., Pancost, R.D., Schouten, S., Singano, J.M., Wade, B.S., 2007. Stable warm tropical climate through the Eocene Epoch. Geology 35, 211–214.

Pearson, P.N., McMillan, I.K., Singano, J.M., Wade, B.S., Jones, T.D., Coxall, H.K., Bown, P.R., Lear, C.H., 2008. Extinction and environmental change across the Eocene–Oligocene boundary in Tanzania. Geology 36, 179–182.

Petrizzo, M.R., 2001. Late Cretaceous planktonic foraminifera from Kerguelen Plateau (ODP Leg 183): new data to improve the Southern Ocean biozonation. Cretaceous Research 22, 829–855.

Petrizzo, M.R., 2002. Palaeoceanographic and palaeoclimatic inferences from Late Cretaceous planktonic foraminiferal assemblages from the Exmouth Plateau (ODP sites 762 and 763, eastern Indian Ocean). Marine Micropaleontology 45, 117–150.

Petrizzo, M.R., 2003. Late Cretaceous planktonic foraminiferal bioevents in the Tethys and in the Southern Ocean record: an overview. Journal of Foraminiferal Research 33, 330–337.

Petrizzo, M.R., Falzoni, F., Premoli Silva, I., 2011. Identification of the base of the lower-to-middle Campanian *Globotruncana ventricosa* Zone: comments on reliability and global correlations. Cretaceous Research 32, 387–405.

Robaszynski, F., Caron, M., 1995. Foraminifères planktoniques du Crétacé: commentaire de la zonation Europe-Méditerranée. Société géologique de France 166, 681–692.

Salman, G., Abdula, I., 1995. Development of the Mozambique and Ruvuma sedimentary basins, offshore Mozambique. Sedimentary Geology 96, 7–41.

Schlüter, T., 1997. Geology of East Africa. Borntraeger, Stuttgart, 512 p.

Serra-Kiel, J., Hottinger, L., Caus, E., Drobne, K., Ferrandez, C., Jauhri, A.K., Less, G., Pavlovec, R., Pignatti, J., Samso, J.M., Schaub, H., Sirel, E., Strougo, A., Tambareau, Y., Tosquella, J., Zakrevskaya, E., 1998. Larger foraminiferal biostratigraphy of the Tethyan Paleocene and Eocene. Bulletin de la Société Géologique de France 169, 281–299.

Sliter, W.V., 1989. Biostratigraphic zonation for Cretaceous planktonic foraminifers examined in thin section. Journal of Foraminiferal Research 19, 1–19.

Stewart, D.R.M., Pearson, P.N., Ditchfield, P.W., Singano, J.M., 2004. Miocene tropical Indian Ocean temperatures: evidence from three exceptionally preserved foraminiferal assemblages in Tanzania. Journal of African Earth Sciences 40, 173–190.

van Dongen, B.E., Talbot, H.M., Schouten, S., Pearson, P.N., Pancost, R.D., 2006. Well preserved Palaeogene and Cretaceous biomarkers from the Kilwa area, Tanzania. Organic Geochemistry 37, 539–557.

Varol, O., 1998. Paleogene. In: Bown, P.R. (Ed.), Calcareous Nannofossil Biostratigraphy. Kluwer Academic, London, pp. 200–224.

Wendler, J., Gräfe, K.U., Willems, H., 2002. Palaeoecology of calcareous dinoflagellate cysts in the mid-Cenomanian Boreal Realm: implications for the reconstruction of palaeoceanography of the NW European shelf sea. Cretaceous Research 23, 213–229.

Wendler, I., Huber, B.T., MacLeod, K.G., Wendler, J.E., 2011. Early evolutionary history of *Tubulogenerina* and *Colomia*: new species from exceptionally preserved Turonian sediments from East Africa. Journal of Foraminiferal Research 41, 384–400.